Electronic Supplementary Information (ESI)

Molecular Engineering of Bis(triphenylamine)-Modified Fluorene Luminophore for Immensely Enriching Anisotropic Force-Triggered High-Contrast Tricolor Fluorescent Molecular Switches Library

Zhao Chen,*[a] Yijie Zou,[a] Ya Yin,[b] Diandian Deng,[d] Yue Yang,[c] Congbin Fan,[a] Shouzhi Pu,*[a] and Gang Liu[a]

[a] Jiangxi Provincial Key Laboratory of Organic Functional Molecules; Institute of Organic Chemistry, Jiangxi Science and Technology Normal University, Nanchang 330013, P. R. China. E-mail: 1020160936@jxstnu.edu.cn; pushouzhi@tsinghua.org.cn

[b] State Key Laboratory of Coordination Chemistry, School of Chemistry and Chemical Engineering, Nanjing University, Nanjing 210023, P. R. China.

[c] College of Chemistry, Jilin University, Changchun 130012, P. R. China.

[d] School of Chemistry and Molecular Engineering, East China Normal University, Shanghai 200241, P. R. China.

Table of Contents

1. Materials/ General Methods/ Instrumentation

All synthetic experiments were carried out under an argon atmosphere applying standard Schlenk techniques. The reactive substances 2,7-dibromo-9*H*-fluoren-9-one, (4-methoxyphenyl)boronic acid, (3-methoxyphenyl)boronic acid, (2-methoxyphenyl)boronic acid, (4-(dimethylamino)phenyl)boronic acid, (3-(dimethylamino)phenyl)boronic acid, (2-(dimethylamino)phenyl)boronic acid, (4-(trifluoromethyl)phenyl)boronic acid, (3-(trifluoromethyl)phenyl)boronic acid, (2-(trifluoromethyl)phenyl)boronic acid, (4-nitrophenyl)boronic acid, (3-nitrophenyl)boronic acid, (2-nitrophenyl)boronic acid, (4-chlorophenyl)boronic acid, (3-chlorophenyl)boronic acid, (2-chlorophenyl)boronic acid, and (4-(diphenylamino)phenyl)boronic acid were purchased directly from Innochem (Beijing, China). All the other reactive substances and all reagents were commercially available and used without further purification. Deuterated solvents were purchased from Cambridge Isotope Laboratory (Andover, MA). TLC analysis was performed using pre-coated glass plates. Column chromatography was performed using silica gel (200-300 mesh). Intermediates **I-1** to **I-15** and **II-1** to **II-15** were prepared by the synthesis methods described in our previously reported literature.[1] ^{1}H NMR and ^{13}C NMR spectra were recorded on a Varian INOVA-500 NMR Spectrometer. ^{1}H NMR spectra were reported as followed: chemical shift in ppm (δ) relative to the chemical shift of TMS at 0.00 ppm, integration, multiplicities (s = singlet, d = doublet, t = triplet, m = multiplet), and coupling constant (Hz). ^{13}C NMR chemical shifts reported in ppm (δ) relative to the central line of triplet for $CDCl_3$ at 77 ppm. High-Resolution Mass Spectrometer (HRMS) spectra were recorded with a Bruker UltrafleXtreme MALDI-TOF/TOF Mass Spectrometer, DHB as matrix. The X-ray crystal-structure determinations of **Sym-*o*-OMe** crystal and **Sym-*o*-NO_2** crystal were carried out on a Bruker APEX DUO CCD system, and their corresponding crystallographic data of **Sym-*o*-OMe** and **Sym-*o*-NO_2** have been deposited in the Cambridge Crystallographic Data Centre as supplemental publications CCDC 2432608 (**Sym-*o*-OMe**) and CCDC 2432609 (**Sym-*o*-NO_2**). Photoluminescence (PL) spectra were measured by a PL spectrometer FLS1000 (Edinburgh Instruments). Powder X-ray diffraction (XRD) data were recorded on a Shimadzu XRD-6000 diffractometer using Ni-filtered and graphite-monochromated Cu Kα radiation (λ = 1.54 Å, 40 kV, 30 mA). Differential scanning

calorimetry data were recorded on Simultaneous Thermal Analyzer (HENVEN, HSC-4PLUS). Density functional theory (DFT) calculations were carried out using Gaussian 16 programs throughout this manuscript. The optimizations of positions of H atoms in single-crystal XRD data were performed using B3LYP hybrid functional[2] with Grimme's dispersion correction of D3 version (Becke-Johnson damping)[3]. The standard 6-31G* basis set[4,5] for all atoms was used. It is said that the reasonable HOMO-LUMO gaps can be obtained at this theoretical level.[6] The isosurfaces of canonical molecular orbitals are obtained by Multiwfn[7] and VMD[8] program. Time-dependent density functional theory (TD-DFT) calculations of **Sym-*o*-OMe** crystal and **Sym-*o*-NO_2** crystal in tetramer forms were performed using the Gaussian 16 program[9]. These calculations were carried out in the gas phase at the TD-B3LYP-D3BJ[10]/6-31G*[11] level of theory, based on the optimized structures. Photographs were recorded on a smart phone (iPhone 14 Pro). The quick response (QR) code was designed according to IEC 18004, and the corresponding information was read out by scanning the QR code under 365 nm UV light via the WeChat APP software of a smart phone (iPhone 14 Pro), which was downloaded for free from the Apple App Store. The information code corresponding to "Bidirectional high-contrast mechanofluorochromism" was registered on www.colorzip.com and read out by a smart phone (iPhone 14 Pro) using the COLORCODE™ APP software, which could also be downloaded for free from the Apple App Store during the completion of this work. This WeChat and COLORCODE™ APP softwares were applied only for exploring QR code-based or 3D-colored code-based anti-counterfeiting applications of **Sym-*p*-OMe** and **Sym-*m*-OMe** and not for any other purposes. The absolute fluorescence quantum yields were measured by a FLS1000 fluorescence spectrophotometer (Edinburgh Instruments) using an integrating sphere and a continuous xenon lamp (450 W) as an excitation source. The fluorescence lifetimes were measured by the FLS1000 spectrofluorometer using a 375 nm EPL picosecond pulsed diode laser.

2. The syntheses of 15 Sym-*Pos*-R compounds

Syntheses of target molecules Sym-*Pos*-R. Compounds **Sym-*Pos*-R** were synthesized in a similar manner. Taking the synthetic procedure of **Sym-*p*-OMe** as a representative example: A mixture of intermediate **II-1** (1.29 mmol, 0.71 g), (4-

(diphenylamino)phenyl)boronic acid (2.70 mmol), Na_2CO_3 (12.8 mmol), $Pd(PPh_3)_4$ (0.26 mmol) were stirred in THF (80 mL) and H_2O (8 mL) for two days under an argon atmosphere at 80°C. After completion of the reaction, the mixture was extracted with dichloromethane and water, and then washed with brine three times. The combined organic layers were dried over anhydrous $MgSO_4$, and concentrated under vacuum. The residual mixture was purified by column chromatography on silica gel using the petroleum ether/dichloromethane (5:1) as eluent, affording the desired pale-yellow solid product **Sym-*p*-OMe** in a good yield of 76%.

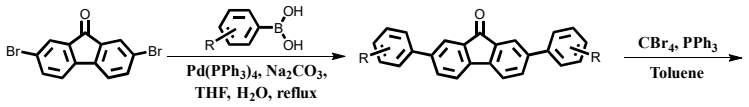

R = *p*-OMe, I-1; R = *p*-NMe_2, I-2; R = *p*-CF_3, I-3; R = *p*-NO_2, I-4; R = *p*-Cl, I-5; R = *m*-OMe, I-6; R = *m*-NMe_2, I-7; R = *m*-CF_3, I-8; R = *m*-NO_2, I-9; R = *m*-Cl, I-10; R = *o*-OMe, I-11; R = *o*-NMe_2, I-12; R = *o*-CF_3, I-13; R = *o*-NO_2, I-14; R = *o*-Cl, I-15

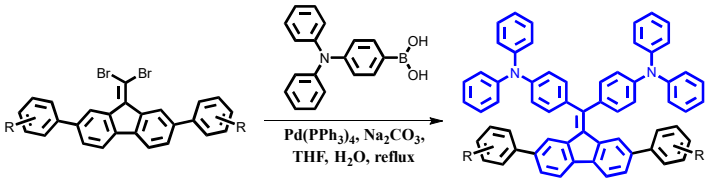

R = *p*-OMe, II-1; R = *p*-NMe_2, II-2; R = *p*-CF_3, II-3; R = *p*-NO_2, II-4; R = *p*-Cl, II-5; R = *m*-OMe, II-6; R = *m*-NMe_2, II-7; R = *m*-CF_3, II-8; R = *m*-NO_2, II-9; R = *m*-Cl, II-10; R = *o*-OMe, II-11; R = *o*-NMe_2, II-12; R = *o*-CF_3, II-13; R = *o*-NO_2, II-14; R = *o*-Cl, II-15

R = *p*-OMe, Sym-*p*-OMe; R = *p*-NMe_2, Sym-*p*-NMe_2; R = *p*-CF_3, Sym-*p*-CF_3; R = *p*-NO_2, Sym-*p*-NO_2; R = *p*-Cl, Sym-*p*-Cl; R = *m*-OMe, Sym-*m*-OMe; R = *m*-NMe_2, Sym-*m*-NMe_2; R = *m*-CF_3, Sym-*m*-CF_3; R = *m*-NO_2, Sym-*m*-NO_2; R = *m*-Cl, Sym-*m*-Cl; R = *o*-OMe, Sym-*o*-OMe; R = *o*-NMe_2, Sym-*o*-NMe_2; R = *o*-CF_3, Sym-*o*-CF_3; R = *o*-NO_2, Sym-*o*-NO_2; R = *o*-Cl, Sym-*o*-Cl

Scheme S1 Synthetic routes of **15 Sym-*Pos*-R compounds**.

Sym-*p*-OMe (Pale-yellow solid; Yield = 76%): ^{1}H NMR (500 MHz, $CDCl_3$): δ (ppm) = 7.68 (d, *J* = 10.0 Hz, 2H), 7.34 (d, *J* = 5.0 Hz, 4H), 7.22 (d, *J* = 10.0 Hz, 4H), 7.19-7.14 (m, 12H), 7.07 (d, *J* = 10.0 Hz, 8H), 7.03-6.96 (m, 8H), 6.91 (d, *J* = 10.0 Hz, 4H), 3.77 (s, 6H). ^{13}C NMR (125 MHz, $CDCl_3$): δ (ppm) = 158.9, 148.2, 147.4, 146.1, 140.1, 138.5, 138.5, 136.1, 134.4, 133.4, 131.7, 129.4, 128.1, 127.9, 125.7, 125.0, 124.8, 123.4, 123.2, 122.3, 119.5, 114.2, 55.4. HRMS-ESI (m/z): Found: $[M + H]^+$ 877.3791; "molecular formula $C_{64}H_{48}N_2O_2$" requires $[M + H]^+$ 877.3789.

Sym-*m*-OMe (Yellow solid; Yield = 78%): ^{1}H NMR (500 MHz, $CDCl_3$): δ (ppm) = 7.72 (d, *J* = 10.0 Hz, 2H), 7.45 (d, *J* = 10.0 Hz, 2H), 7.29 (t, *J* = 10.0 Hz, 2H), 7.23-7.12 (m, 16H), 7.06-6.94 (m, 18H), 6.83-6.81 (m, 2H), 3.75 (s, 6H). ^{13}C NMR (125 MHz, $CDCl_3$): δ (ppm) = 158.9, 148.2, 147.3, 146.1, 140.0, 138.5, 138.4, 136.1, 134.4, 131.7, 129.4,

128.1, 127.9, 125.7, 125.0, 124.8, 123.4, 123.3, 123.2, 122.2, 119.5, 114.1, 55.3. HRMS-ESI (m/z): Found: $[M + H]^+$ 877.3781; "molecular formula $C_{64}H_{48}N_2O_2$" requires $[M + H]^+$ 877.3789.

Sym-*o*-OMe (Pale-yellow solid; Yield = 75%): ^{1}H NMR (500 MHz, $CDCl_3$): δ (ppm) = 7.75 (d, *J* = 10.0 Hz, 2H), 7.49 (d, *J* = 5.0 Hz, 2H), 7.34-7.31 (m, 2H), 7.27 (d, *J* = 10.0 Hz, 5H), 7.24 (d, *J* = 1.5 Hz, 1H), 7.16 (t, *J* = 7.5 Hz, 8H), 7.11 (s, 2H), 7.06-6.97 (m, 20H), 3.77 (s, 6H). ^{13}C NMR (125 MHz, $CDCl_3$): δ (ppm) = 156.4, 147.9, 147.4, 145.4, 139.3, 138.9, 136.5, 136.2, 134.0, 131.3, 131.2, 130.7, 129.3, 128.8, 128.3, 126.0, 124.8, 123.1, 122.6, 120.9, 118.7, 111.2, 55.5. HRMS-ESI (m/z): Found: $[M + H]^+$ 877.3793; "molecular formula $C_{64}H_{48}N_2O_2$" requires $[M + H]^+$ 877.3789.

Sym-*p*-NMe$_2$ (Yellow solid; Yield = 71%): ^{1}H NMR (500 MHz, $CDCl_3$): δ (ppm) = 7.65 (d, *J* = 10.0 Hz, 2H), 7.40 (d, *J* = 10.0 Hz, 2H), 7.31 (d, *J* = 10.0 Hz, 4H), 7.23 (d, *J* = 10.0 Hz, 4H), 7.19-7.08 (m, 20H), 7.03 (d, *J* = 5.0 Hz, 4H), 6.96 (t, *J* = 7.5 Hz, 4H), 6.75 (s, 2H), 2.92 (s, 12H). ^{13}C NMR (125 MHz, $CDCl_3$): δ (ppm) = 149.7, 148.1, 147.4, 145.5, 140.0, 138.7, 138.2, 136.44, 133.8, 131.6, 130.9, 129.9, 129.3, 128.8, 127.4, 125.3, 125.0, 123.3, 122.8, 122.4, 119.3, 112.9, 40.7. HRMS-ESI (m/z): Found: $[M + H]^+$ 903.4422; "molecular formula $C_{66}H_{54}N_4$" requires $[M + H]^+$ 903.4422.

Sym-*m*-NMe$_2$ (Orange-red solid; Yield = 73%): ^{1}H NMR (500 MHz, $CDCl_3$): δ (ppm) = 7.71 (d, *J* = 10.0 Hz, 2H), 7.46 (d, *J* = 5.0 Hz, 2H), 7.23 (d, *J* = 10.0 Hz, 4H), 7.19 (s, 4H), 7.16-7.11 (m, 10H), 7.02-6.94 (m, 16H), 6.78-6.67 (m, 4H), 2.91 (s, 12H). ^{13}C NMR (125 MHz, $CDCl_3$): δ (ppm) = 148.2, 147.3, 146.0, 142.8, 140.0, 139.9, 138.9, 136.1, 133.5, 131.4, 129.3, 129.0, 127.5, 126.4, 125.1, 123.9, 123.3, 122.8, 122.2, 121.8, 119.4, 116.2, 115.6, 111.4, 111.3, 40.7. HRMS-ESI (m/z): Found: $[M + H]^+$ 903.4421; "molecular formula $C_{66}H_{54}N_4$" requires $[M + H]^+$ 903.4422.

Sym-*o*-NMe$_2$ (Orange-yellow solid; Yield = 70%): ^{1}H NMR (500 MHz, $CDCl_3$): δ (ppm) = 7.73 (d, *J* = 10.0 Hz, 2H), 7.54 (d, *J* = 5.0 Hz, 2H), 7.27 (d, *J* = 10.0 Hz, 3H), 7.24 (d, *J* = 10.0 Hz, 3H), 7.17 (t, *J* = 7.5 Hz, 8H), 7.13-7.05 (m, 6H), 7.02 (d, *J* = 5.0 Hz, 18H), 2.53 (d, *J* = 20.0 Hz, 12H). ^{13}C NMR (125 MHz, $CDCl_3$): δ (ppm) = 151.1, 147.9, 147.4, 145.4, 139.9, 139.6, 138.4, 136.4, 134.5, 133.9, 131.5, 131.2, 129.3, 129.3, 127.9, 127.8, 125.2, 124.9, 124.2, 123.2, 122.5, 121.2, 118.9, 117.3, 43.4. HRMS-ESI (m/z): Found: $[M + H]^+$ 903.4418; "molecular formula $C_{66}H_{54}N_4$" requires $[M + H]^+$ 903.4422.

Sym-*p*-CF_3 (Yellow-green solid; Yield = 81%): ^{1}H NMR (500 MHz, $CDCl_3$): δ (ppm) = 7.79 (d, *J* = 5.0 Hz, 2H), 7.63 (d, *J* = 5.0 Hz, 4H), 7.51 (d, *J* = 10.0 Hz, 4H), 7.24-7.15 (m, 20H), 7.02 (t, *J* = 15.0 Hz, 12H). ^{13}C NMR (125 MHz, $CDCl_3$): δ (ppm) = 148.6, 147.2, 145.3, 139.4, 137.6, 131.8, 129.4, 129.1, 128.9, 128.6, 127.6, 127.1, 126.2, 125.7, 125.7, 125.6, 125.4, 125.1, 123.7, 123.2, 122.1, 121.1, 119.9. HRMS-ESI (m/z): Found: $[M + H]^+$ 953.3334; "molecular formula $C_{64}H_{42}F_6N_2$" requires $[M + H]^+$ 953.3325.

Sym-*m*-CF_3 (Orange-red solid; Yield = 76%): ^{1}H NMR (500 MHz, $CDCl_3$): δ (ppm) = 7.78 (d, *J* = 10.0 Hz, 2H), 7.68 (s, 2H), 7.57-7.47 (m, 6H), 7.21 (t, *J* = 10.0 Hz, 10H), 7.12 (t, *J* = 7.5 Hz, 8H), 6.99 (t, *J* = 10.0 Hz, 14H). ^{13}C NMR (125 MHz, $CDCl_3$): δ (ppm) = 148.6, 147.1, 142.6, 139.1, 137.6, 131.7, 131.5, 131.2, 131.0, 130.7, 130.1, 129.3, 129.2, 127.4, 126.1, 125.2, 123.8, 123.8, 123.6, 123.1, 121.7, 120.9, 120.0. HRMS-ESI (m/z): Found: $[M + H]^+$ 953.3332; "molecular formula $C_{64}H_{42}F_6N_2$" requires $[M + H]^+$ 953.3325.

Sym-*o*-CF_3 (Orange-yellow solid; Yield = 80%): Its ^{1}H NMR, ^{13}C NMR and HRMS data and spectra can be found in our previously reported literature.[1]

Sym-*p*-NO_2 (Orange-red solid; Yield = 65%): ^{1}H NMR (500 MHz, $CDCl_3$): δ (ppm) = 8.29 (d, *J* = 5.0 Hz, 2H), 7.83-7.77 (m, 2H), 7.59 (d, *J* = 10.0 Hz, 2H), 7.54-7.52 (m, 1H), 7.33-7.26 (m, 10H), 7.24-7.20 (m, 10H), 7.12-7.02 (m, 15H). ^{13}C NMR (125 MHz, $CDCl_3$): δ (ppm) = 148.5, 148.4, 147.2, 147.1, 147.0, 146.6, 140.6, 140.0, 139.7, 139.2, 136.1, 135.7, 135.6, 132.6, 131.8, 131.7, 129.4, 129.4, 127.4, 127.2, 126.0, 125.1, 125.0, 124.6, 124.0, 123.9, 123.7, 123.6, 122.1, 122.0, 119.8, 119.7. HRMS-ESI (m/z): Found: $[M + H]^+$ 907.3274; "molecular formula $C_{62}H_{42}N_4O_4$" requires $[M + H]^+$ 907.3279.

Sym-*m*-NO_2 (Orange-red solid; Yield = 63%): ^{1}H NMR (500 MHz, $CDCl_3$): δ (ppm) = 8.35 (t, *J* = 2.5 Hz, 1H), 8.18-8.16 (m, 1H), 7.83 (d, *J* = 5.0 Hz, 1H), 7.77 (t, *J* = 7.5 Hz, 2H), 7.60-7.52 (m, 2H), 7.33-7.26 (m, 9H), 7.25-7.17 (m, 11H), 7.11-7.01 (m, 15H). ^{13}C NMR (125 MHz, $CDCl_3$): δ (ppm) = 148.8, 148.4, 148.3, 147.3, 147.2, 146.9, 143.6, 140.2, 140.1, 139.6, 139.3, 136.2, 135.8, 135.7, 132.8, 132.6, 131.6, 131.6, 129.5, 129.4, 129.3, 127.2, 126.6, 125.9, 125.0, 125.0, 124.6, 123.6, 123.5, 122.2, 122.1, 121.7, 119.8. HRMS-ESI (m/z): Found: $[M + H]^+$ 907.3278; "molecular formula $C_{62}H_{42}N_4O_4$" requires $[M + H]^+$ 907.3279.

Sym-*o*-NO_2 (Yellow solid; Yield = 62%): ^{1}H NMR (500 MHz, $CDCl_3$): δ (ppm) = 7.87 (d, *J*

= 10.0 Hz, 2H), 7.79 (d, *J* = 5.0 Hz, 2H), 7.62 (t, *J* = 7.5 Hz, 2H), 7.49 (t, *J* = 7.5 Hz, 2H), 7.38 (d, *J* = 10.0 Hz, 2H), 7.24-7.18 (m, 14H), 7.03 (t, *J* = 10.0 Hz, 16H), 6.94 (s, 2H). ^{13}C NMR (125 MHz, $CDCl_3$): δ (ppm) = 149.1, 148.3, 147.6, 147.3, 139.8, 139.3, 137.1, 135.6, 135.3, 132.5, 132.2, 132.0, 131.4, 129.3, 127.8, 126.8, 125.0, 124.4, 124.3, 123.3, 122.5, 119.7. HRMS-ESI (m/z): Found: $[M + H]^+$ 907.3271; "molecular formula $C_{62}H_{42}N_4O_4$" requires $[M + H]^+$ 907.3279.

Sym-*p*-Cl (Orange-yellow solid; Yield = 78%): ^{1}H NMR (500 MHz, $CDCl_3$): δ (ppm) = 7.73-7.66 (m, 2H), 7.41-7.37 (m, 2H), 7.32 (d, *J* = 10.0 Hz, 4H), 7.24-7.12 (m, 18H), 7.08-6.98 (m, 16H). ^{13}C NMR (125 MHz, $CDCl_3$): δ (ppm) = 148.5, 147.3, 147.3, 140.3, 140.2, 139.0, 137.8, 135.8, 133.0, 131.7, 131.7, 131.6, 129.4, 129.3, 128.9, 128.1, 125.9, 125.3, 125.1, 125.1, 125.0, 124.7, 123.6, 123.5, 123.5, 122.3, 122.2, 119.8. HRMS-ESI (m/z): Found: $[M + H]^+$ 885.2794; "molecular formula $C_{62}H_{42}Cl_2N_2$" requires $[M + H]^+$ 885.2798.

Sym-*m*-Cl (Yellow solid; Yield = 75%): ^{1}H NMR (500 MHz, $CDCl_3$): δ (ppm) = 7.81 (d, *J* = 5.0 Hz, 2H), 7.50-7.47 (m, 4H), 7.38-7.27 (m, 10H), 7.23-7.18 (m, 10H), 7.13-7.03 (m, 16H). ^{13}C NMR (125 MHz, $CDCl_3$): δ (ppm) = 148.6, 147.2, 147.2, 143.7, 140.3, 139.2, 137.6, 135.4, 134.7, 132.7, 131.7, 129.9, 139.4, 127.1, 126.9, 126.0, 125.3, 125.3, 125.0, 125.0, 123.6, 123.6, 123.5, 121.8, 119.8. HRMS-ESI (m/z): Found: $[M + H]^+$ 885.2808; "molecular formula $C_{62}H_{42}Cl_2N_2$" requires $[M + H]^+$ 885.2798.

Sym-*o*-Cl (Yellow solid; Yield = 73%): ^{1}H NMR (500 MHz, $CDCl_3$): δ (ppm) =7.74 (d, *J* = 5.0 Hz, 2H), 7.43 (d, *J* = 5.0 Hz, 2H), 7.33-7.31 (m, 2H), 7.26-7.21 (m, 6H), 7.19 (t, *J* = 2.5 Hz, 6H), 7.13 (t, *J* = 7.5 Hz, 8H), 6.98-6.94 (m, 16H). ^{13}C NMR (125 MHz, $CDCl_3$): δ (ppm) = 148.1, 147.4, 146.7, 141.1, 139.4, 139.1, 137.3, 136.1, 133.2, 132.5, 131.4, 130.0, 129.3, 128.6, 128.3, 126.8, 126.0, 124.9, 124.4, 123.3, 122.6, 118.9. HRMS-ESI (m/z): Found: $[M + H]^+$ 885.2803; "molecular formula $C_{62}H_{42}Cl_2N_2$" requires $[M + H]^+$ 885.2798.

3. Fluorescence responses of luminogens Sym-*m*-NMe_2, Sym-*p*-NO_2, Sym-*m*-NO_2, and Sym-*m*-CF_3 before and after mechanical stimulation

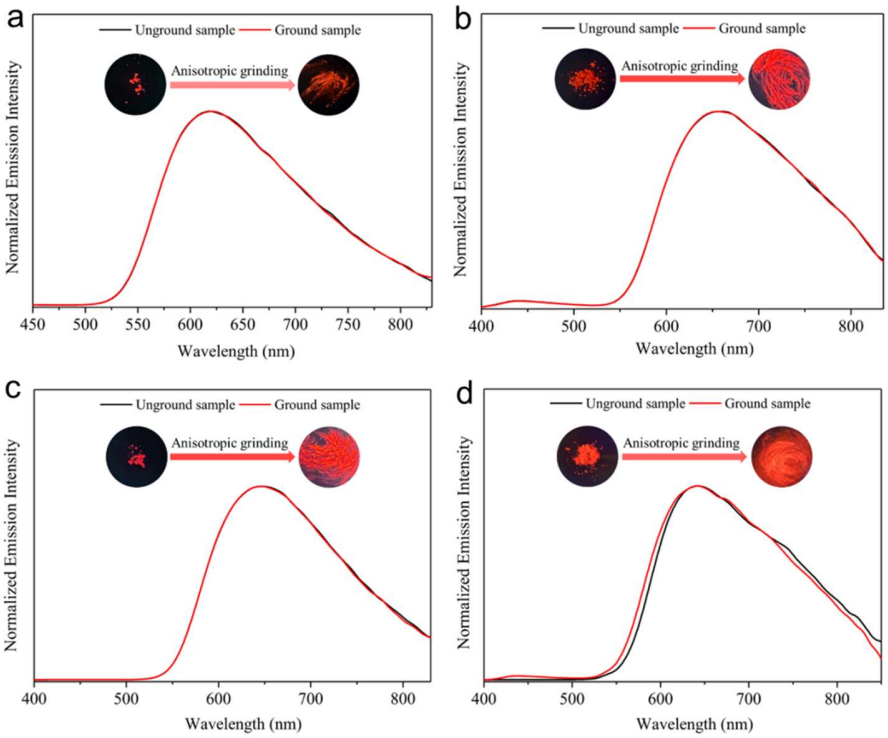

Fig. S1 Normalized PL spectra and PL photographs under 365 nm UV light of solids **Sym-*m*-NMe$_2$** (a), **Sym-*p*-NO$_2$** (b), **Sym-*m*-NO$_2$** (c), and **Sym-*m*-CF$_3$** (d) before and after grinding.

4. Powder XRD patterns of luminogens Sym-*m*-NMe$_2$, Sym-*p*-NO$_2$, Sym-*m*-NO$_2$, and Sym-*m*-CF$_3$ before and after mechanical stimulation

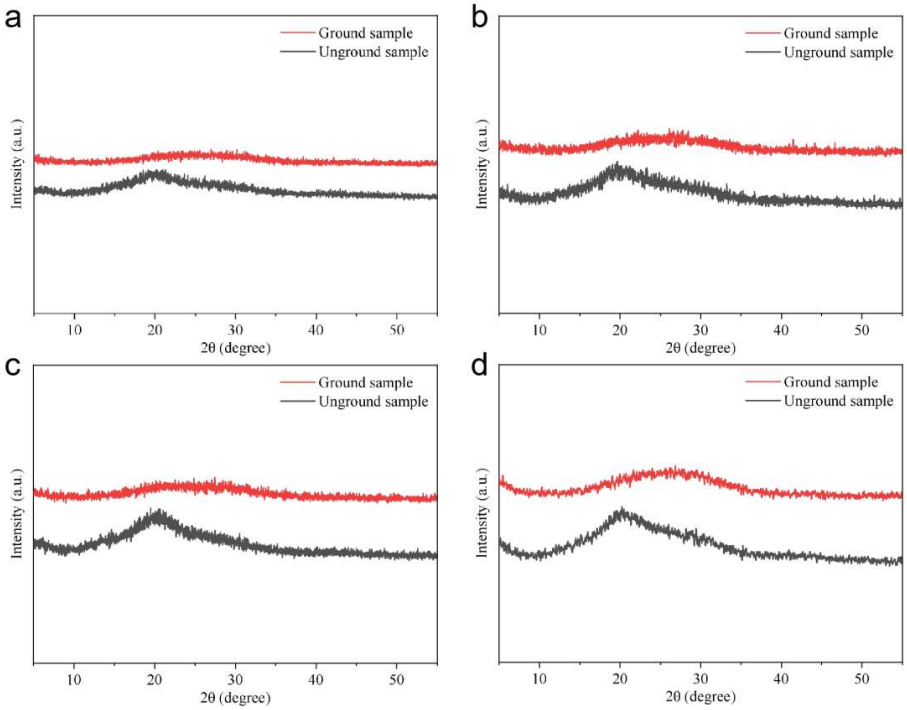

Fig. S2 Powder XRD patterns of solids **Sym-*m*-NMe$_2$** (a), **Sym-*p*-NO$_2$** (b), **Sym-*m*-NO$_2$** (c), and **Sym-*m*-CF$_3$** (d) before and after grinding.

5. The three-color mechanofluorochromic repeatabilities of 10 new developed fluorogenic compounds

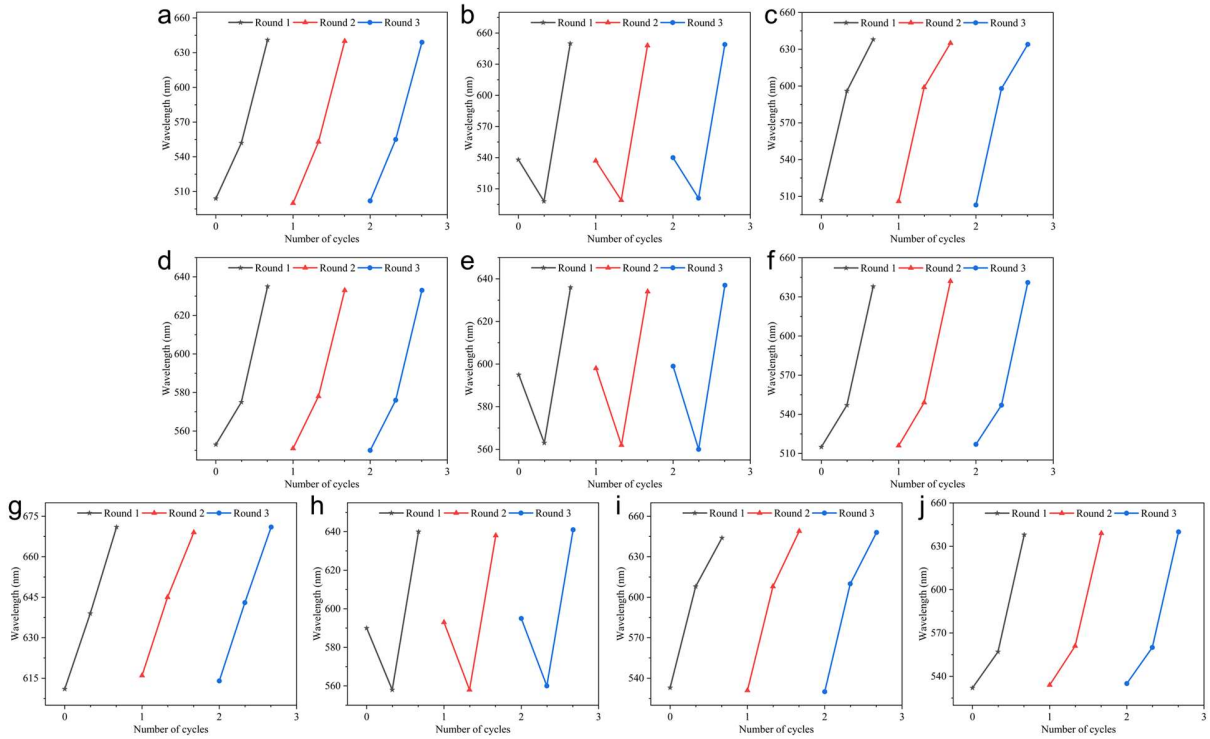

Fig. S3 The repeatability demonstration of three-color mechanofluorochromism of (a) **Sym-*p*-OMe**, (b) **Sym-*m*-OMe**, (c) **Sym-*o*-OMe**, (d) **Sym-*p*-NMe$_2$**, (e) **Sym-*o*-NMe$_2$**, (f) **Sym-*p*-CF$_3$**, (g) **Sym-*o*-NO$_2$**, (h) **Sym-*p*-Cl**, (i) **Sym-*m*-Cl** or (j) **Sym-*o*-Cl**.

6. CIE chromaticity diagrams of various solid states of 14 new Sym-*Pos*-R luminogens

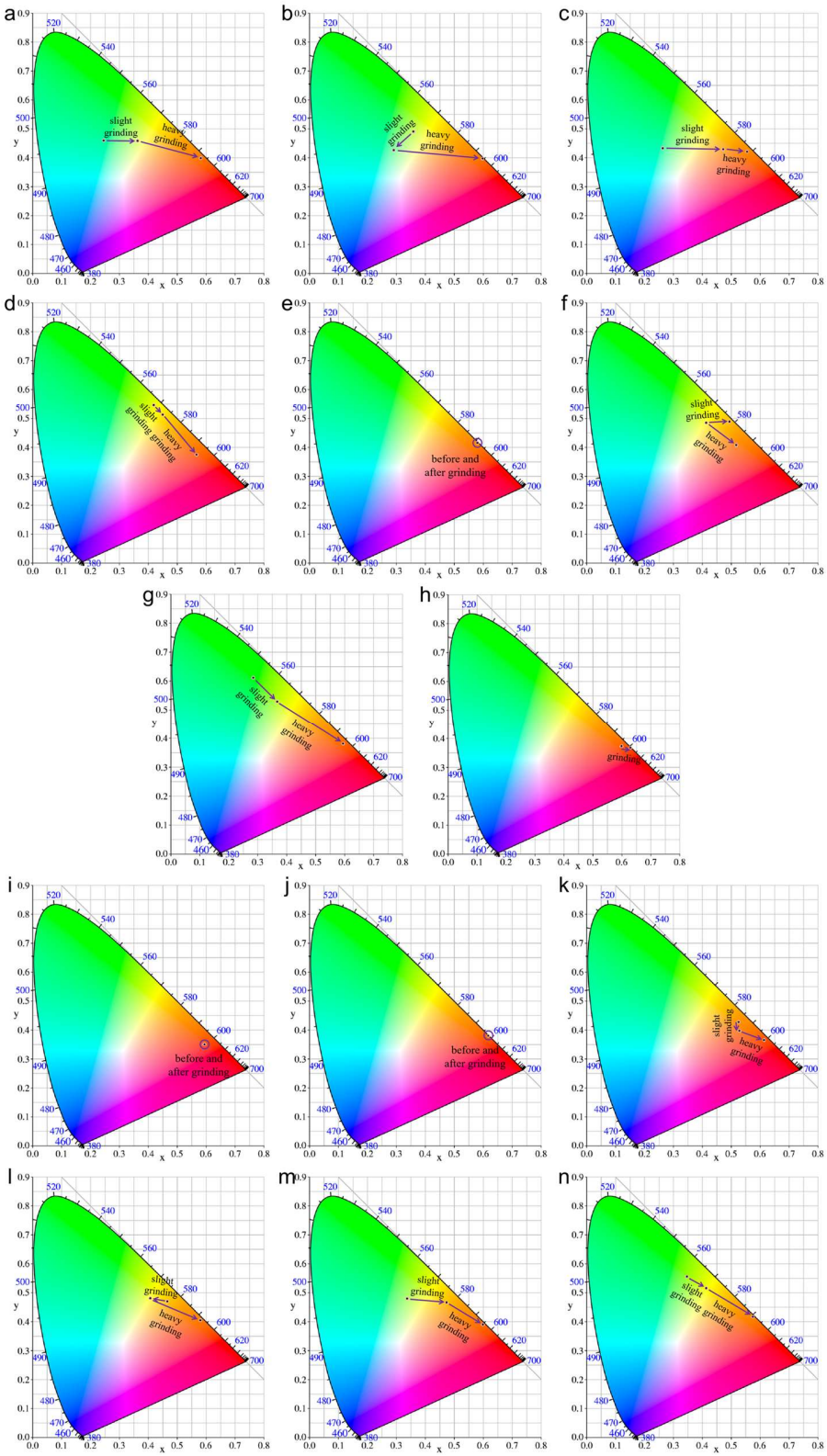

Fig. S4 CIE chromaticity diagrams of 14 new **Sym-*Pos*-R** luminogens in various solid states: (a) **Sym-*p*-OMe**; (b) **Sym-*m*-OMe**; (c) **Sym-*o*-OMe**; (d) **Sym-*p*-NMe$_2$**; (e) **Sym-*m*-NMe$_2$**; (f) **Sym-*o*-**

NMe_2; (g) **Sym-*p*-CF_3**; (h) **Sym-*m*-CF_3**; (i) **Sym-*p*-NO_2**; (j) **Sym-*m*-NO_2**; (k) **Sym-*o*-NO_2**; (l) **Sym-*p*-Cl**; (m) **Sym-*m*-Cl**; (n) **Sym-*o*-Cl**.

7. ^{1}H NMR spectra of various solid forms in $CDCl_3$ of Sym-*m*-OMe, Sym-*o*-OMe or Sym-*p*-NO_2

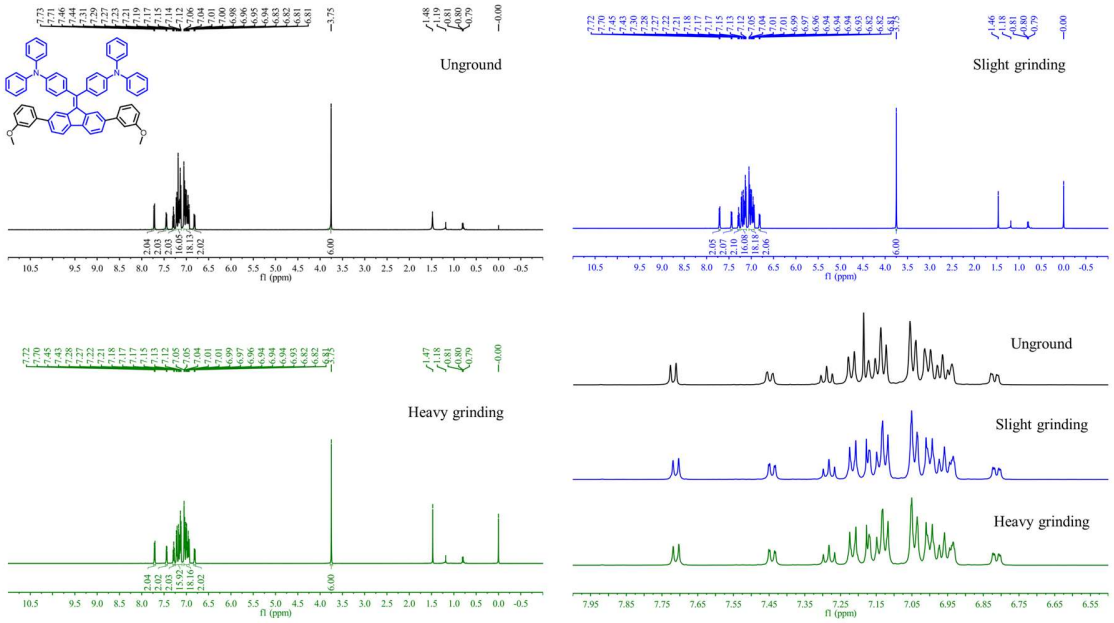

Fig. S5 ^{1}H NMR spectra of pristine, slightly ground, and heavily ground solid samples in $CDCl_3$ of **Sym-*m*-OMe**.

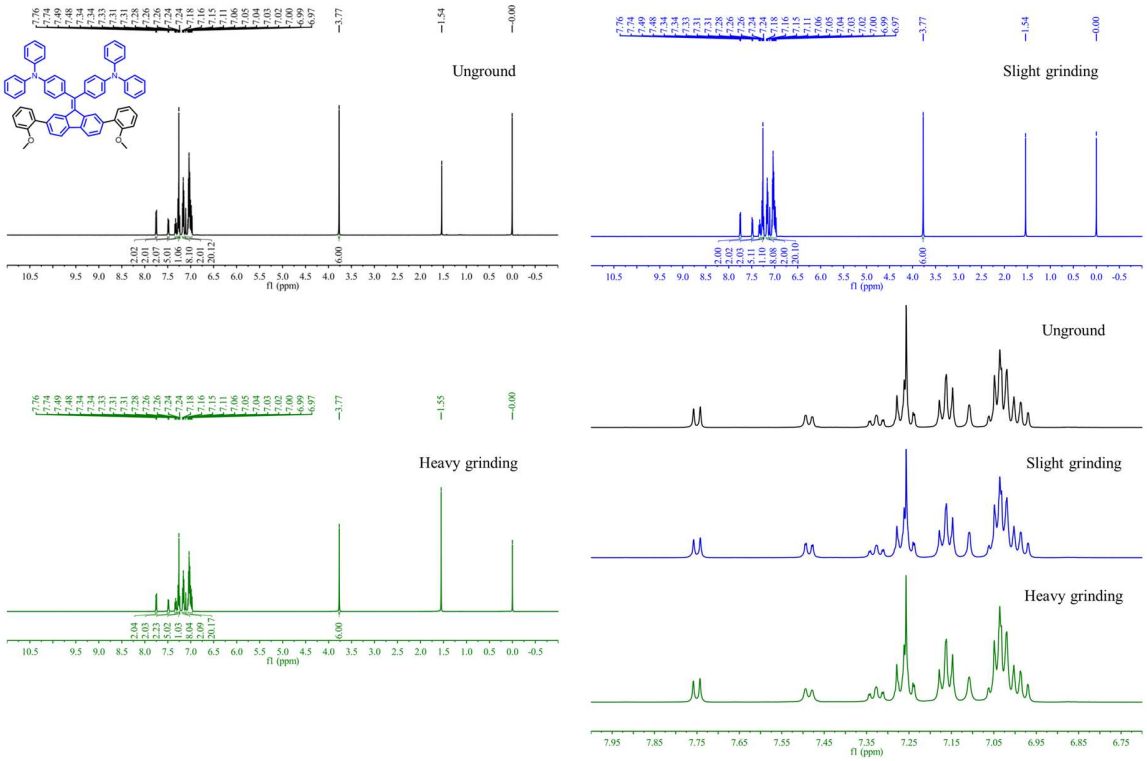

Fig. S6 ^{1}H NMR spectra of pristine, slightly ground, and heavily ground solid samples in $CDCl_3$ of **Sym-*o*-OMe**.

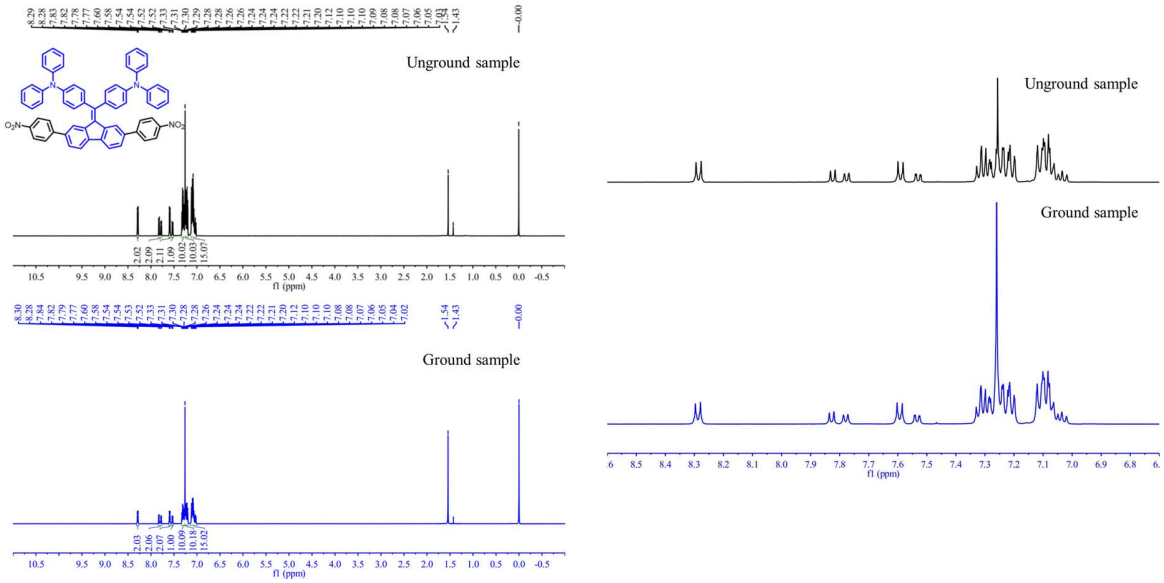

Fig. S7 ^{1}H NMR spectra of pristine and ground solid samples in $CDCl_3$ of **Sym-*p*-NO$_2$**.

8. The average fluorescence lifetimes (τ) of 14 new Sym-*Pos*-R luminogens in different solid states

Table S1 The average τ values of various solid states of 14 new **Sym-*Pos*-R** compounds

Compound	τ /ns (unground)	τ /ns (slight grinding)	τ /ns (heavy grinding)	τ /ns (fuming)
Sym-*p*-OMe	6.18	5.05	1.12	6.08
Sym-*m*-OMe	2.74	2.21	1.22	2.55
Sym-*o*-OMe	9.42	2.14	1.32	9.39
Sym-*p*-NMe_2	4.33	3.91	0.71	4.32
Sym-*m*-NMe_2	1.42	\	1.15	\
Sym-*o*-NMe_2	2.28	1.89	1.14	2.24
Sym-*p*-CF_3	4.04	3.33	1.15	3.98
Sym-*m*-CF_3	1.28	\	1.08	\
Sym-*p*-NO_2	1.39	\	1.25	\
Sym-*m*-NO_2	1.53	\	1.14	\
Sym-*o*-NO_2	3.37	1.98	0.87	3.30
Sym-*p*-Cl	2.99	3.96	1.14	3.12
Sym-*m*-Cl	2.76	2.30	1.07	2.72
Sym-*o*-Cl	3.08	2.73	1.27	3.25

9. Decay curves of different solid forms at maximum emission peaks of 10 new three-color mechanofluorochromic compounds

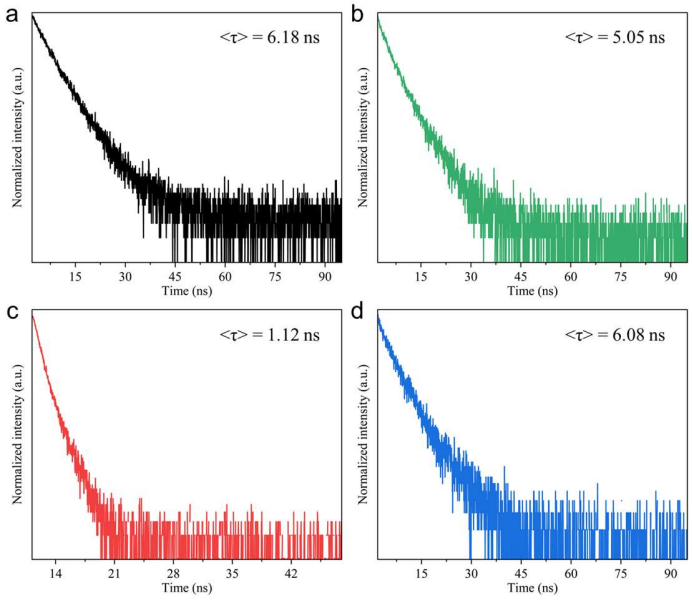

Fig. S8 Decay curves of different solid forms at maximum emission peaks of luminogen **Sym-*p*-OMe**: (a) unground solid; (b) slightly ground solid; (c) heavily ground solid; (d) solid after treatment with dichloromethane. Excitation wavelength: 375 nm.

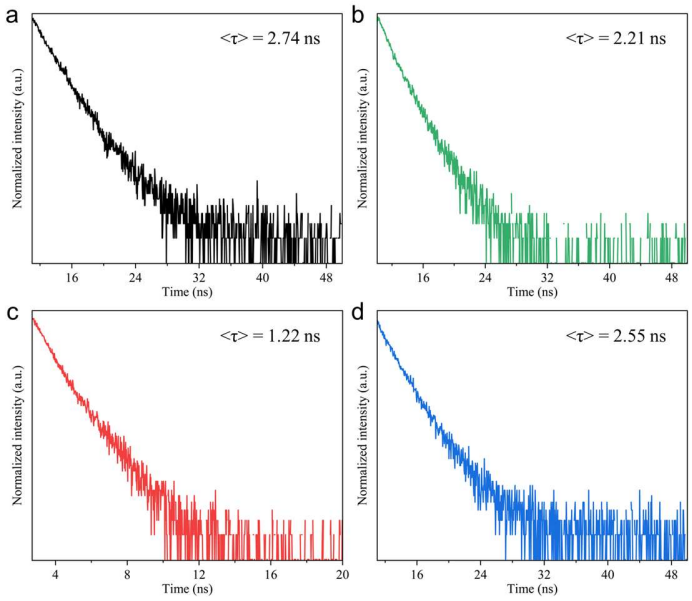

Fig. S9 Decay curves of different solid forms at maximum emission peaks of luminogen **Sym-*m*-OMe**: (a) unground solid; (b) slightly ground solid; (c) heavily ground solid; (d) solid after treatment with dichloromethane. Excitation wavelength: 375 nm.

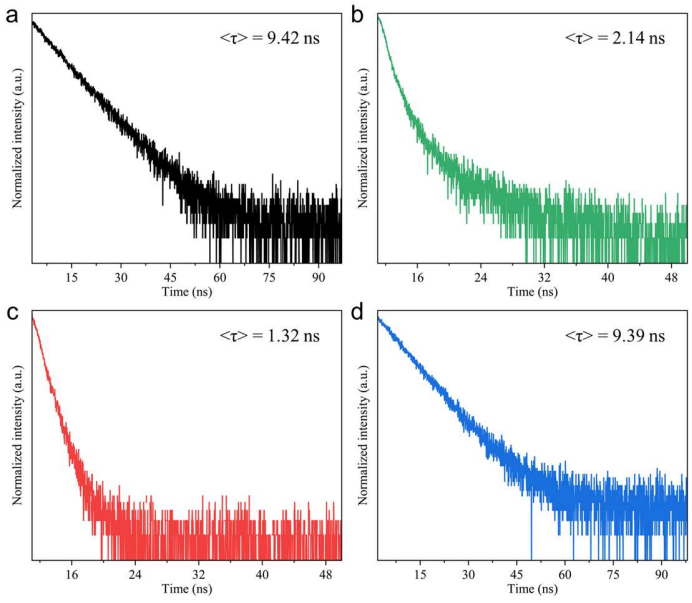

Fig. S10 Decay curves of different solid forms at maximum emission peaks of luminogen **Sym-*o*-OMe**: (a) unground solid; (b) slightly ground solid; (c) heavily ground solid; (d) solid after treatment with dichloromethane. Excitation wavelength: 375 nm.

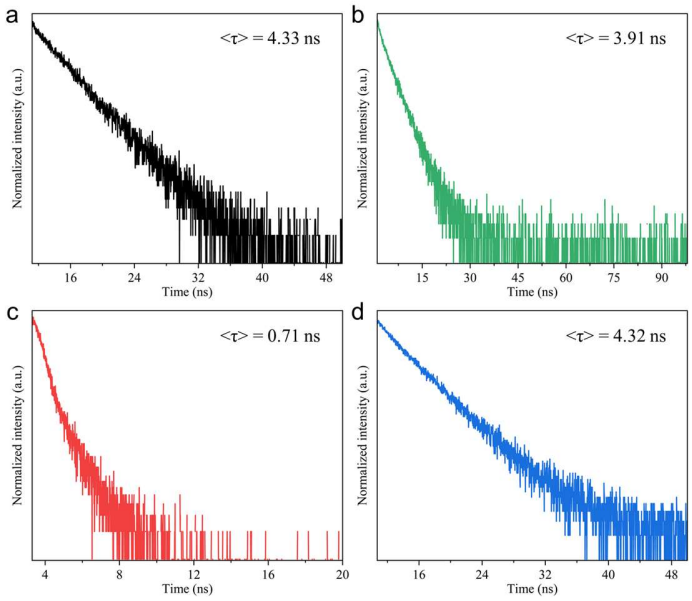

Fig. S11 Decay curves of different solid forms at maximum emission peaks of luminogen **Sym-*p*-NMe$_2$**: (a) unground solid; (b) slightly ground solid; (c) heavily ground solid; (d) solid after treatment with dichloromethane. Excitation wavelength: 375 nm.

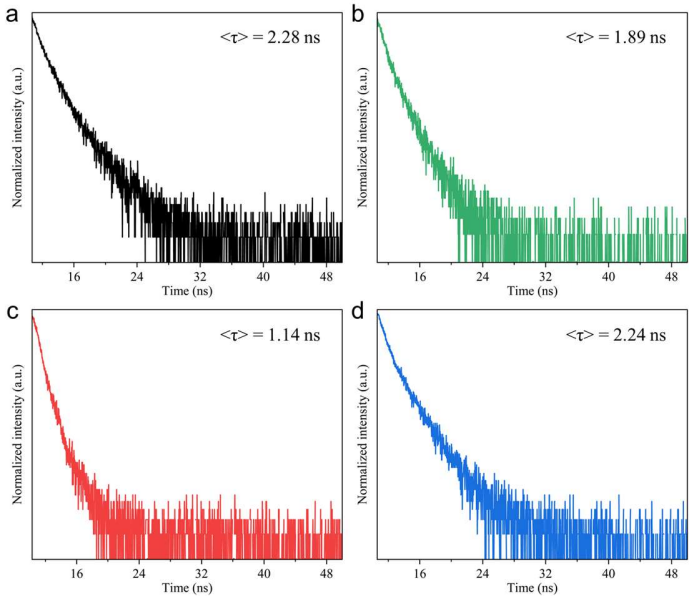

Fig. S12 Decay curves of different solid forms at maximum emission peaks of luminogen **Sym-*o*-NMe$_2$**: (a) unground solid; (b) slightly ground solid; (c) heavily ground solid; (d) solid after treatment with dichloromethane. Excitation wavelength: 375 nm.

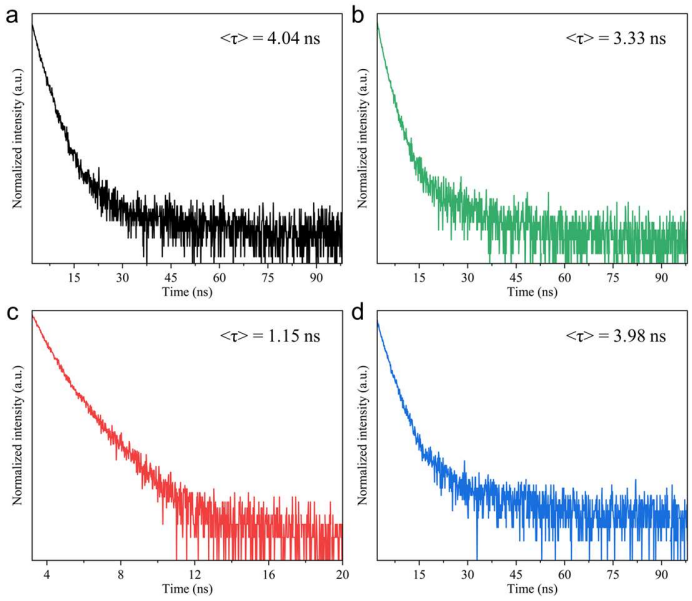

Fig. S13 Decay curves of different solid forms at maximum emission peaks of luminogen **Sym-*p*-CF_3**: (a) unground solid; (b) slightly ground solid; (c) heavily ground solid; (d) solid after treatment with dichloromethane. Excitation wavelength: 375 nm.

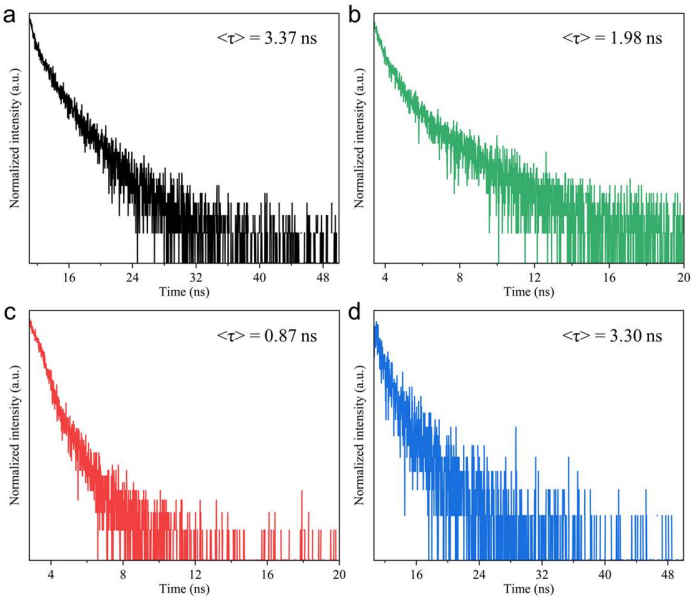

Fig. S14 Decay curves of different solid forms at maximum emission peaks of luminogen **Sym-*o*-NO_2**: (a) unground solid; (b) slightly ground solid; (c) heavily ground solid; (d) solid after treatment with dichloromethane. Excitation wavelength: 375 nm.

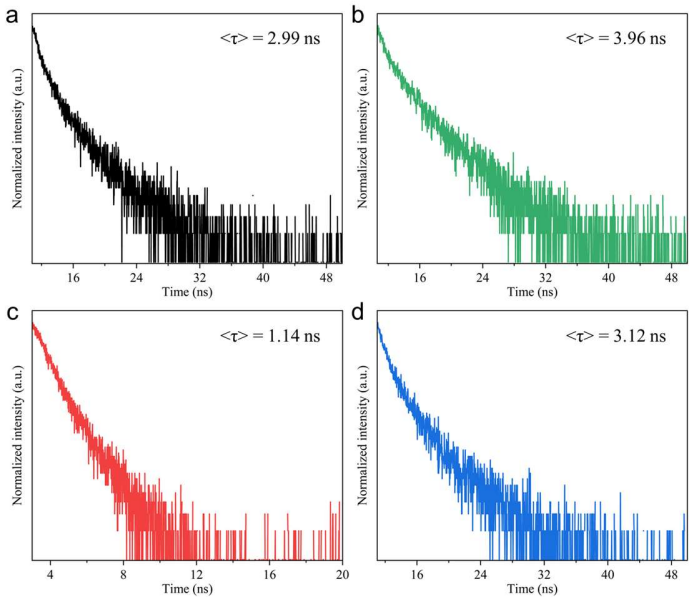

Fig. S15 Decay curves of different solid forms at maximum emission peaks of luminogen **Sym-*p*-Cl**: (a) unground solid; (b) slightly ground solid; (c) heavily ground solid; (d) solid after treatment with dichloromethane. Excitation wavelength: 375 nm.

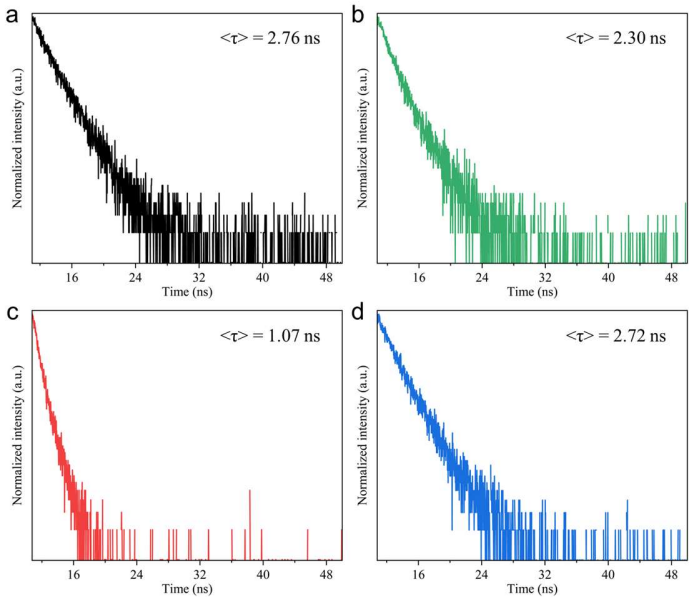

Fig. S16 Decay curves of different solid forms at maximum emission peaks of luminogen **Sym-*m*-Cl**: (a) unground solid; (b) slightly ground solid; (c) heavily ground solid; (d) solid after treatment with dichloromethane. Excitation wavelength: 375 nm.

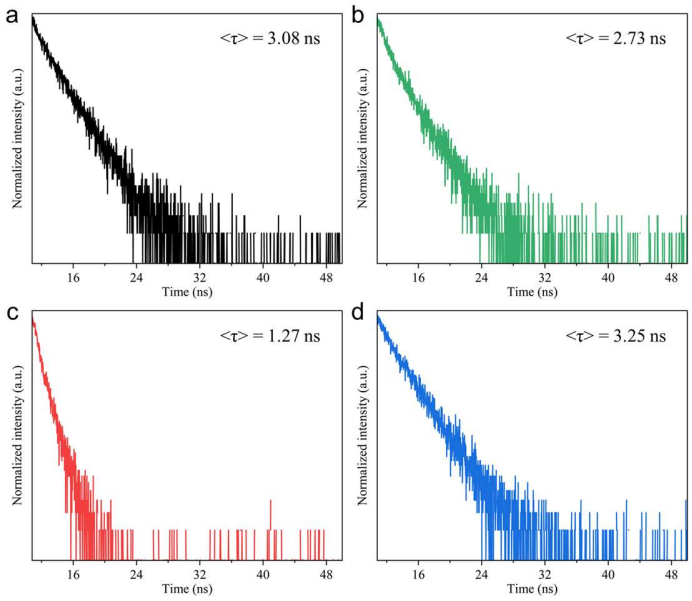

Fig. S17 Decay curves of different solid forms at maximum emission peaks of luminogen **Sym-*o*-Cl**: (a) unground solid; (b) slightly ground solid; (c) heavily ground solid; (d) solid after treatment with dichloromethane. Excitation wavelength: 375 nm.

10. Powder XRD patterns of luminogens Sym-*o*-NMe_2, Sym-*p*-Cl, Sym-*o*-OMe, Sym-*p*-NMe_2, Sym-*p*-CF_3, Sym-*o*-NO_2, Sym-*m*-Cl, and Sym-*o*-Cl in various solid states

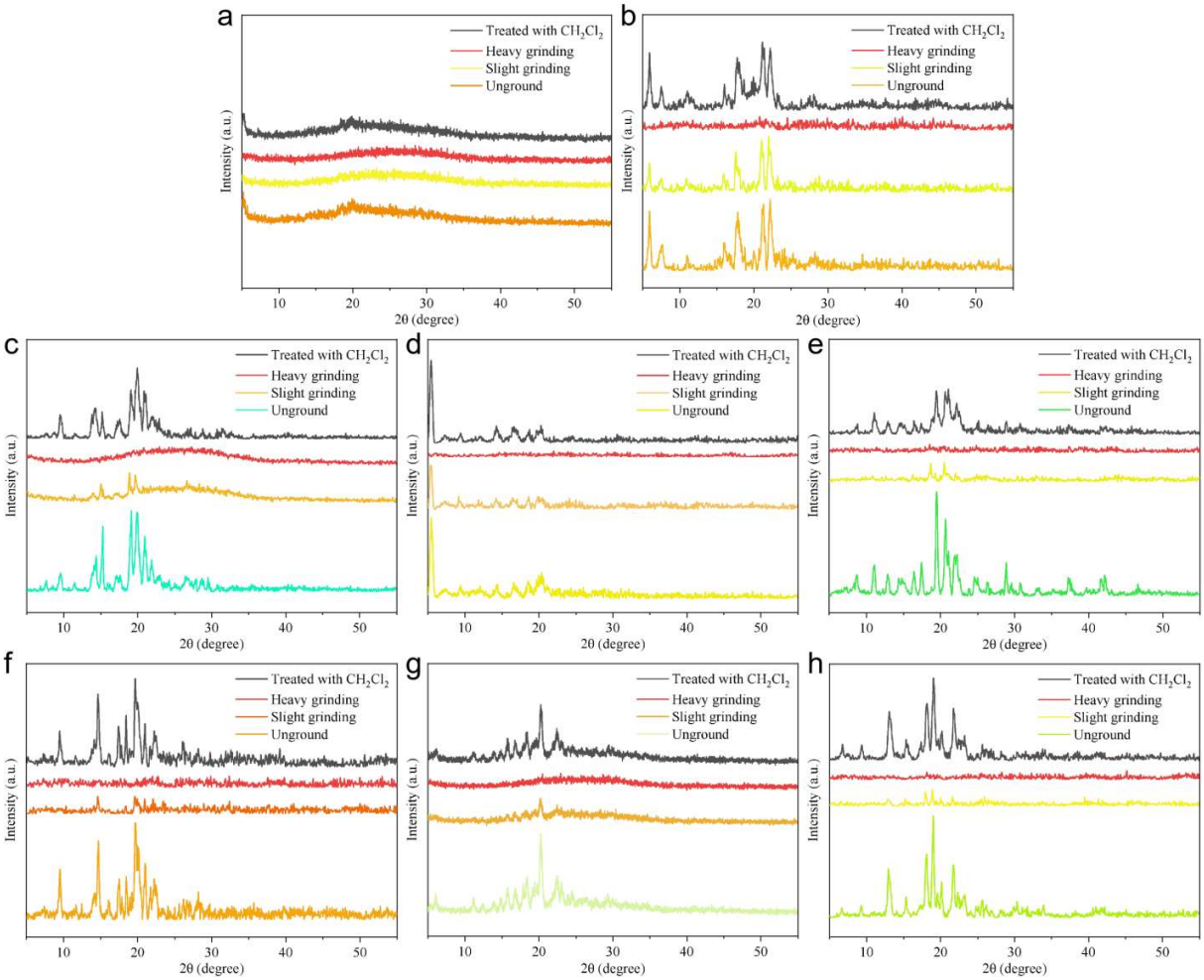

Fig. S18 Powder XRD patterns of various solid states of **Sym-*o*-NMe$_2$** (a), **Sym-*p*-Cl** (b), **Sym-*o*-OMe** (c), **Sym-*p*-NMe$_2$** (d), **Sym-*p*-CF$_3$** (e), **Sym-*o*-NO$_2$** (f), **Sym-*m*-Cl** (g), and **Sym-*o*-Cl** (h).

11. Concentration-dependent fluorescence property of compound Sym-*o*-OMe in CH_2Cl_2 solutions

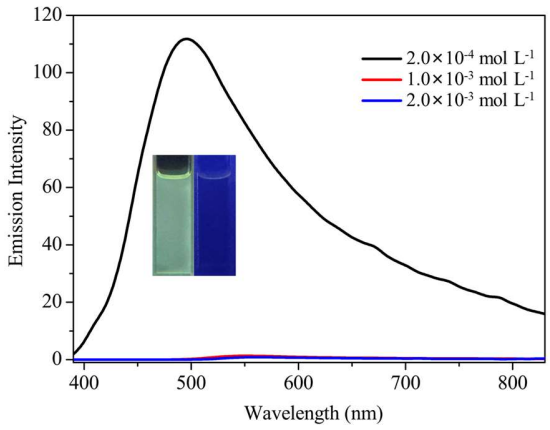

Fig. S19 Fluorescence spectra of compound **Sym-*o*-OMe** in different concentrations of CH_2Cl_2 solutions. Excitation wavelength: 365 nm. The insets show fluorescence photographs under 365 nm UV light of **Sym-*o*-OMe** in different concentrations of CH_2Cl_2 solutions (left: 2.0×10^{-4} mol L^{-1}; right: 1.0×10^{-3} mol L^{-1}).

12. Aggregation-induced emission behavior of compound Sym-*o*-OMe

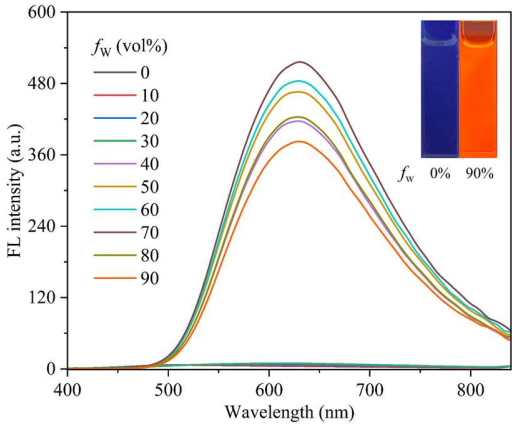

Fig. S20 Fluorescence spectra of compound **Sym-*o*-OMe** (2.0×10^{-5} mol L^{-1}) in DMF/water mixtures with various water fraction (f_w) values. Excitation wavelength = 365 nm. The inset shows the fluorescence images of **Sym-*o*-OMe** (2.0×10^{-5} mol L^{-1}) in pure DMF as well as 90% water fraction under 365 nm UV light.

13. Schematic diagram of molecular packing variation and enhanced intermolecular π-π interactions of solid Sym-*o*-OMe after heavy grinding

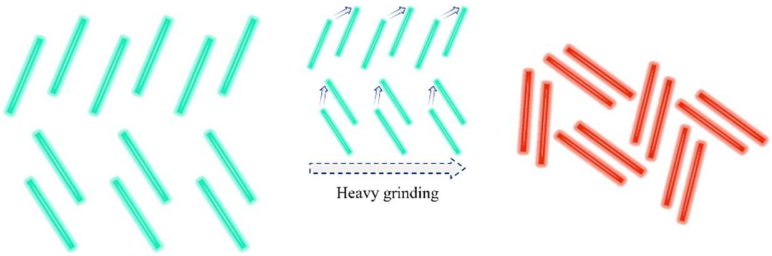

Fig. S21 Schematic diagram of molecular packing variation and enhanced intermolecular π-π interactions of green fluorescent solid **Sym-*o*-OMe** after heavy grinding.

14. Energy diagrams and the frontier molecular orbitals contribution of tetramer forms of Sym-*o*-OMe and Sym-*o*-NO_2

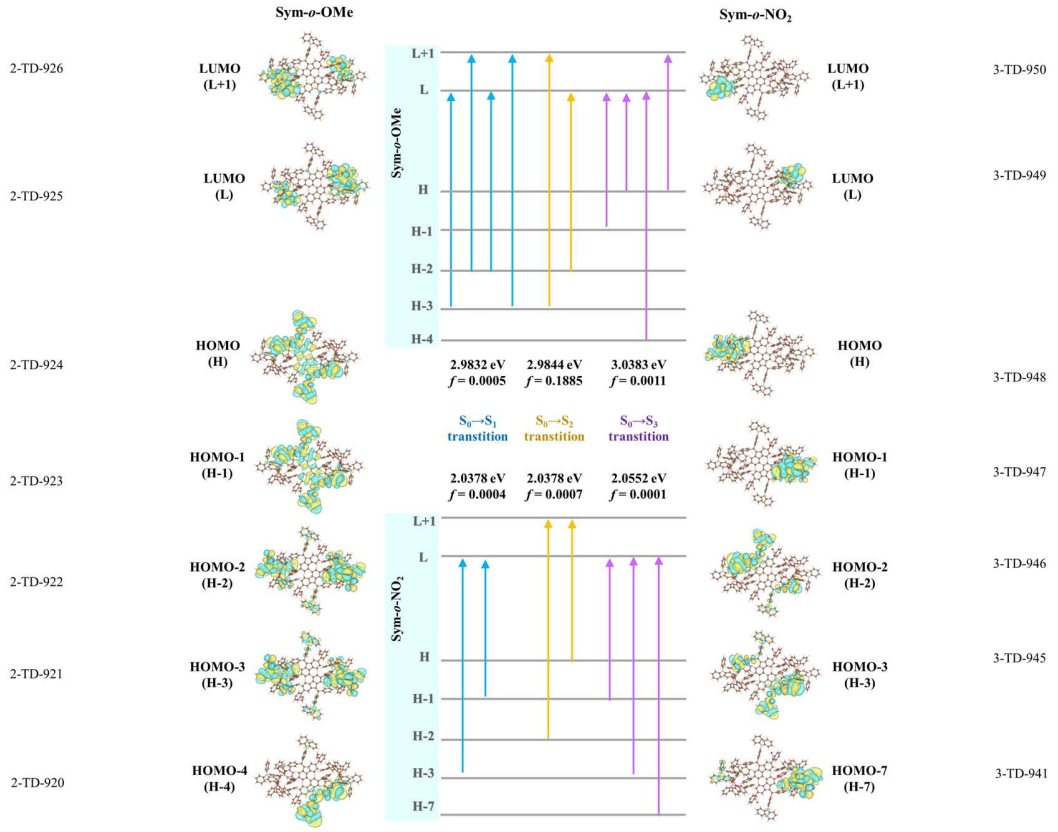

Fig. S22 Energy diagrams and the frontier molecular orbitals contribution of **Sym-*o*-OMe** crystal and **Sym-*o*-NO_2** crystal in tetramer forms.

15. Major eclectronic excitations for tetramer forms of Sym-*o*-OMe and Sym-*o*-NO_2

Table S2 Major eclectronic excitations for **Sym-*o*-OMe** crystal and **Sym-*o*-NO_2** crystal in tetramer forms

	Sym-*o*-OMe		Sym-*o*-NO_2	
S_1	HOMO-3 → LUMO	33.4%	HOMO-3 → LUMO	69.6%
	HOMO-2 → LUMO+1	31.6%	HOMO-1 → LUMO	19.9%
	HOMO-2 → LUMO	16.2%		
	HOMO-3 → LUMO+1	11.1%		
S_2	HOMO-3 → LUMO+1	45.6%	HOMO-2 → LUMO+1	69.7%
	HOMO-2 → LUMO	40.9%	HOMO → LUMO+1	19.7%
S_3	HOMO-1 → LUMO	35.6%	HOMO-1 → LUMO	62.4%
	HOMO → LUMO	32.7%	HOMO-3 → LUMO	21.3%
	HOMO-4 → LUMO	14.6%	HOMO-7 → LUMO	14.6%
	HOMO → LUMO+1	8.8%		

16. Hirshfeld surface analyses and intermolecular C-H···π, C-H···O, and π···π interactions summarizations of molecular packing structures of Sym-*o*-OMe and Sym-*o*-NO_2

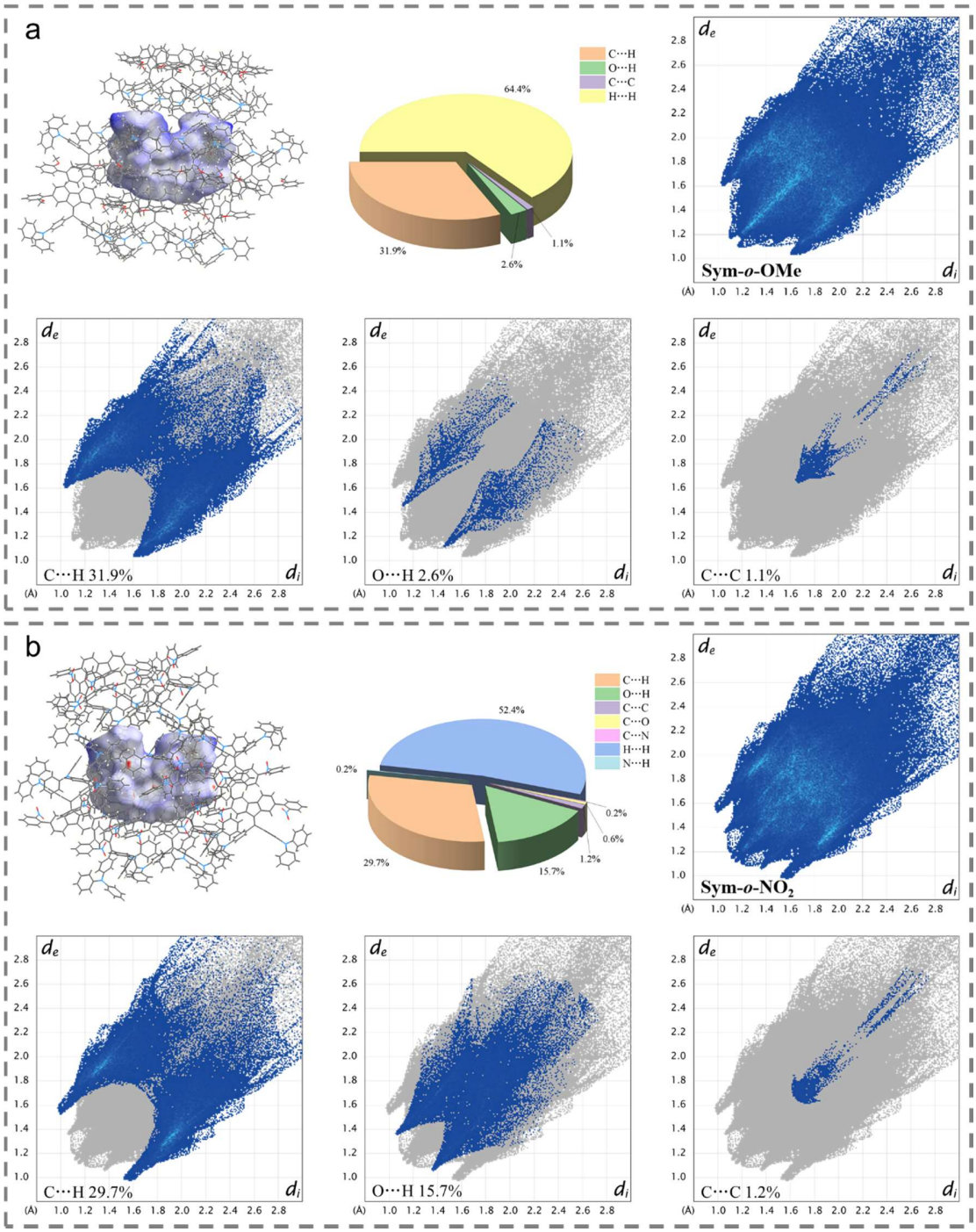

Fig. S23 Hirshfeld surface mapped with the parameter dnorm; pie-chart: relative contributions of various intermolecular interactions to the Hirshfeld surface area; 2-D fingerprint plots of compound: full, and resolved into C···H, O···H and C···C contacts showing the percentages of contacts contributed to the total Hirshfeld surface area of molecule. The grey shadow is an outline of the complete fingerprint plot for each plot. (a) for **Sym-*o*-OMe** and (b) for **Sym-*o*-NO$_2$**.

Table S3 Multiple intermolecular C-H···π, C-H···O, and π···π interactions summarizations of stacking structures of **Sym-*o*-OMe** crystal and **Sym-*o*-NO_2** crystal

	C-H···π	C-H···O	π···π
Sym-*o*-OMe	2.843 Å	2.712 Å	4.080 Å
	2.829 Å		
	2.795 Å		
	2.780 Å		
	2.690 Å		
	2.666 Å		
Sym-*o*-NO_2	2.796 Å	2.714 Å	4.048 Å
	2.743 Å	2.695 Å	
	2.610 Å	2.551 Å	
	2.352 Å	2.543 Å	
	2.348 Å		

17. Tricolor mechanofluorochromic behaviors of luminogens Sym-*p*-NMe_2 and Sym-*o*-NO_2

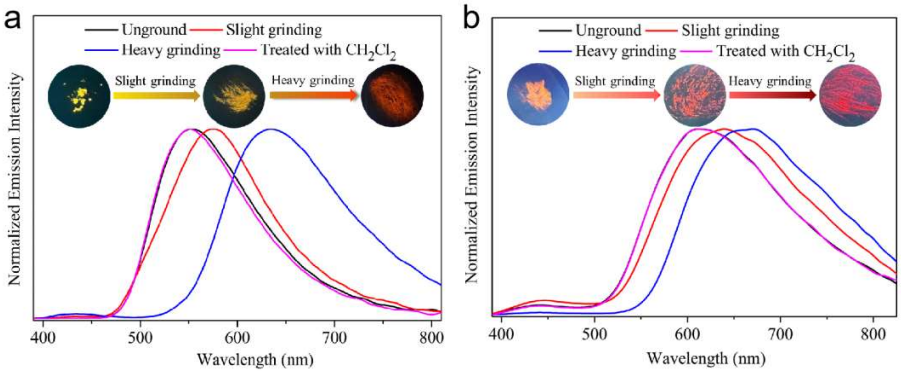

Fig. S24 Normalized PL spectra and PL photographs under 365 nm UV light of **Sym-*p*-NMe_2** (a), **Sym-*o*-NO_2** (b) in various solid states.

18. Copies of NMR spectra and HRMS spectra of 14 new Sym-*Pos*-R compounds

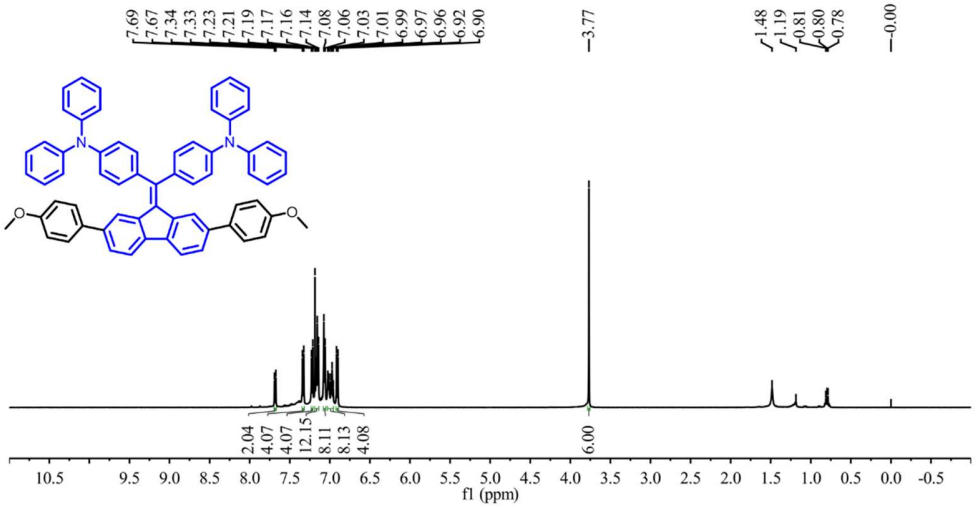

^{1}H NMR spectrum of **Sym-*p*-OMe**

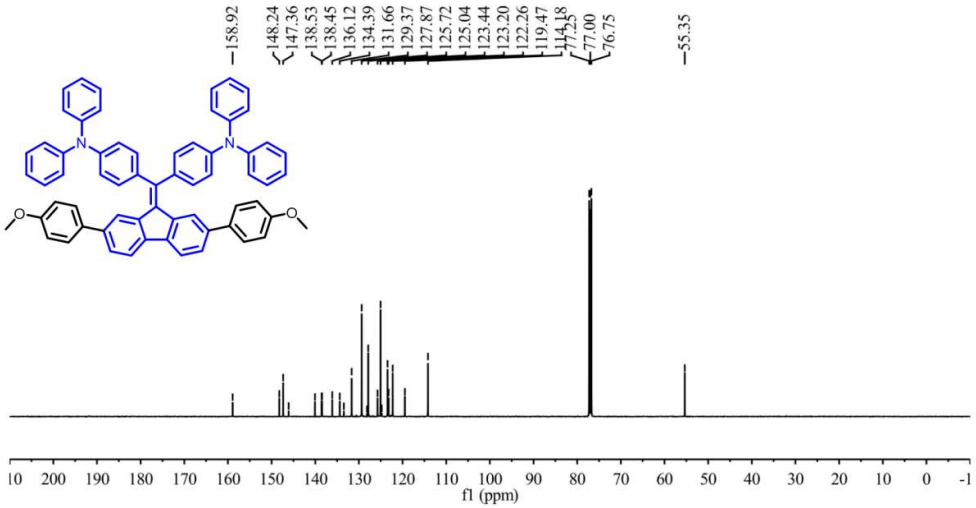

^{13}C NMR spectrum of **Sym-*p*-OMe**

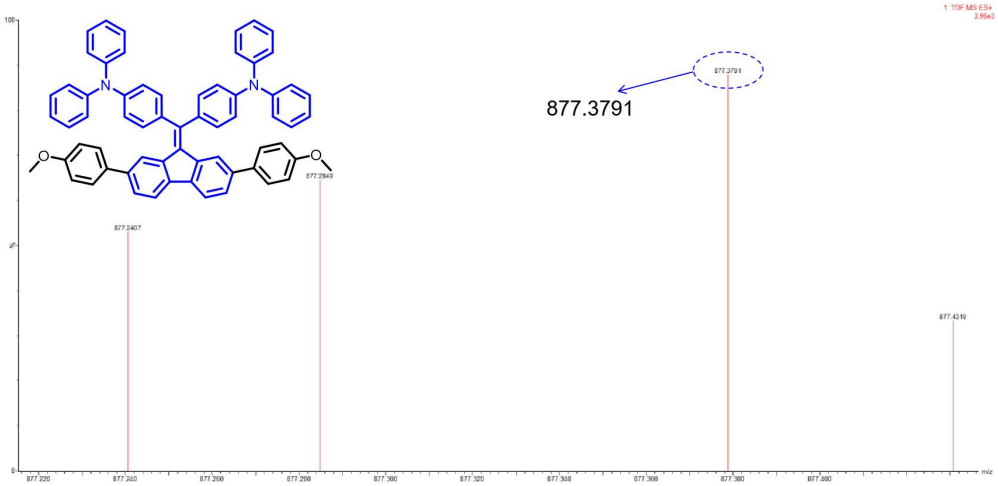

HRMS spectrum of **Sym-*p*-OMe**

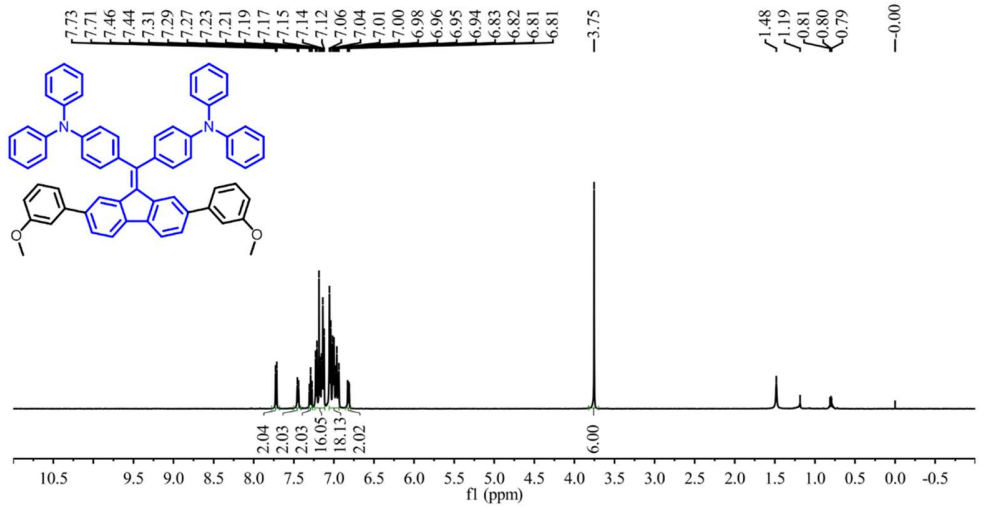

^{1}H NMR spectrum of **Sym-*m*-OMe**

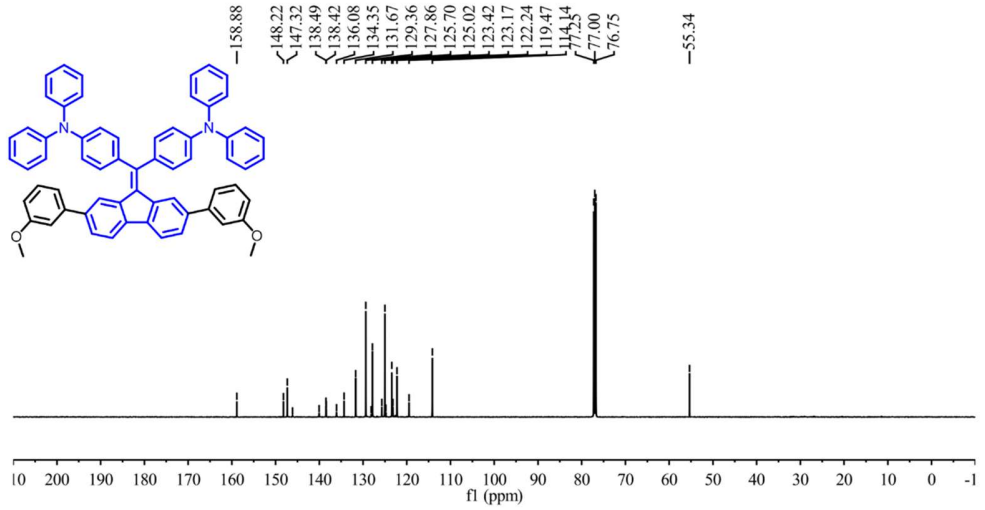

^{13}C NMR spectrum of **Sym-*m*-OMe**

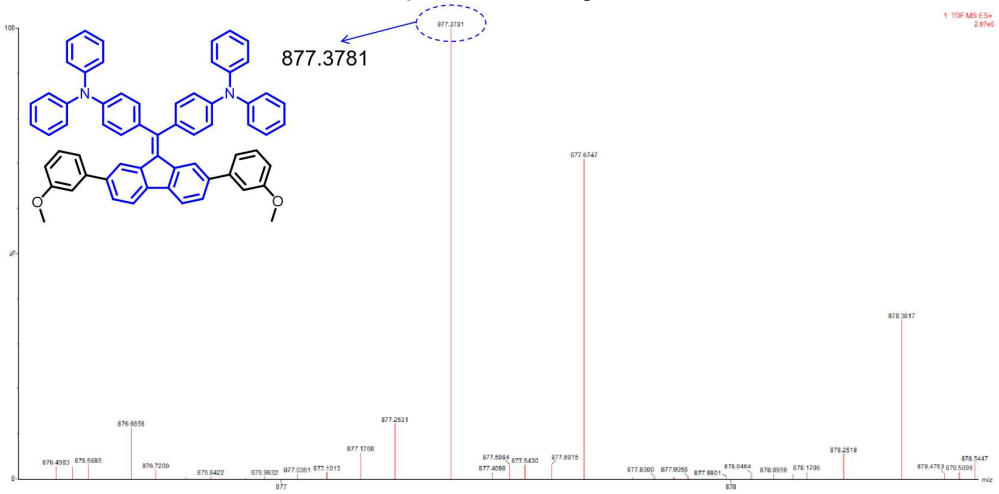

HRMS spectrum of **Sym-*m*-OMe**

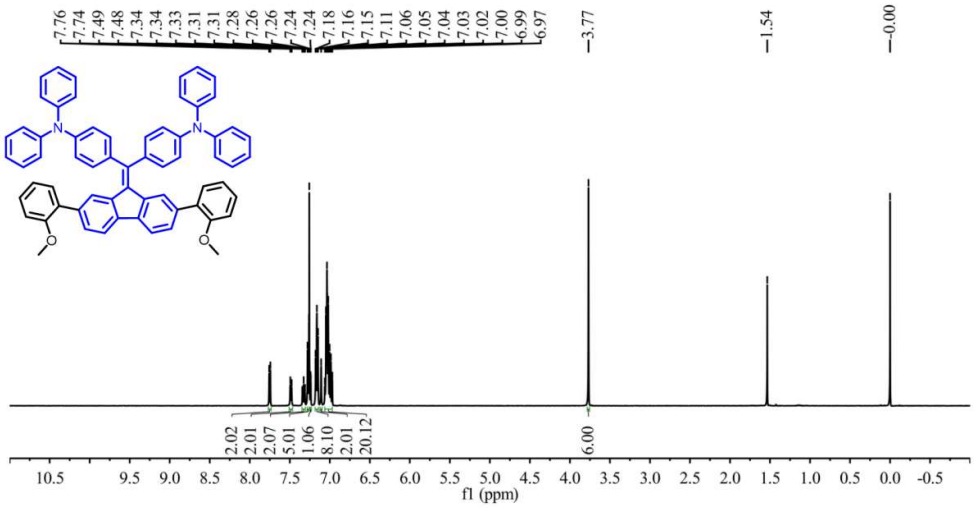

^{1}H NMR spectrum of **Sym-*o*-OMe**

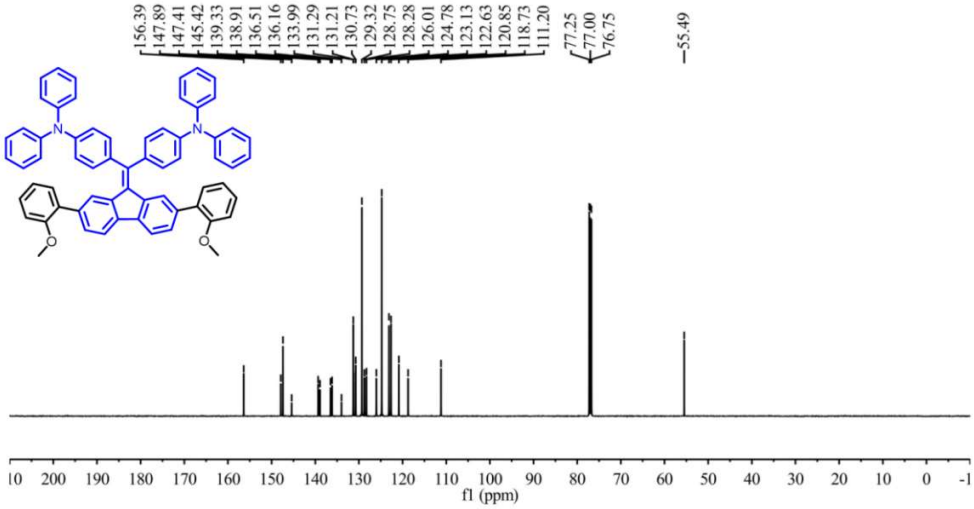

^{13}C NMR spectrum of **Sym-*o*-OMe**

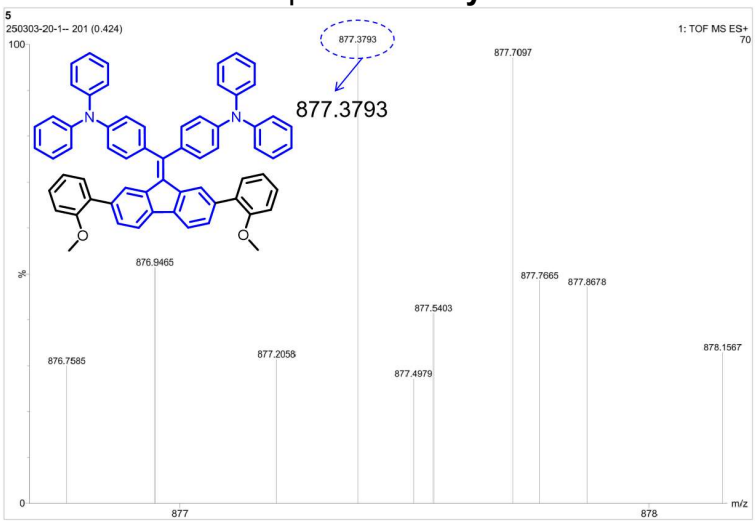

HRMS spectrum of **Sym-*o*-OMe**

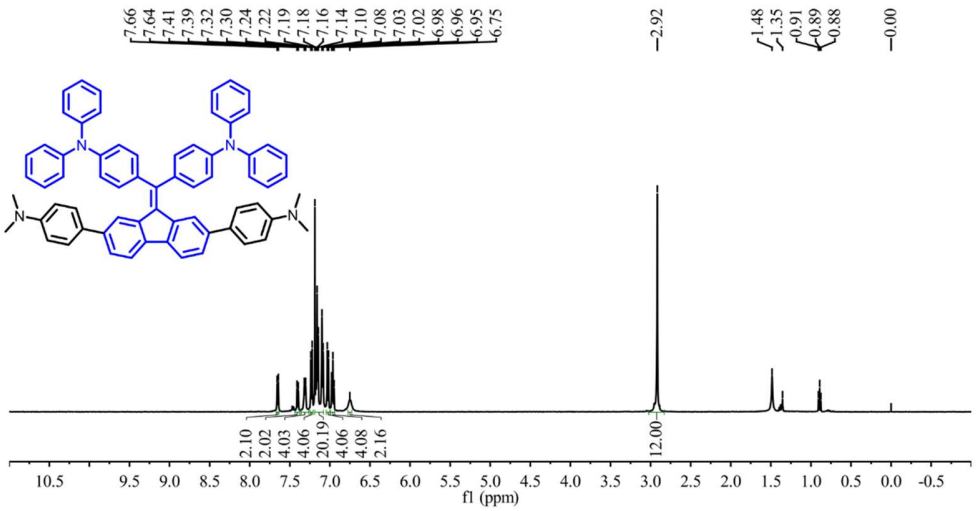

^{1}H NMR spectrum of **Sym-*p*-NMe$_2$**

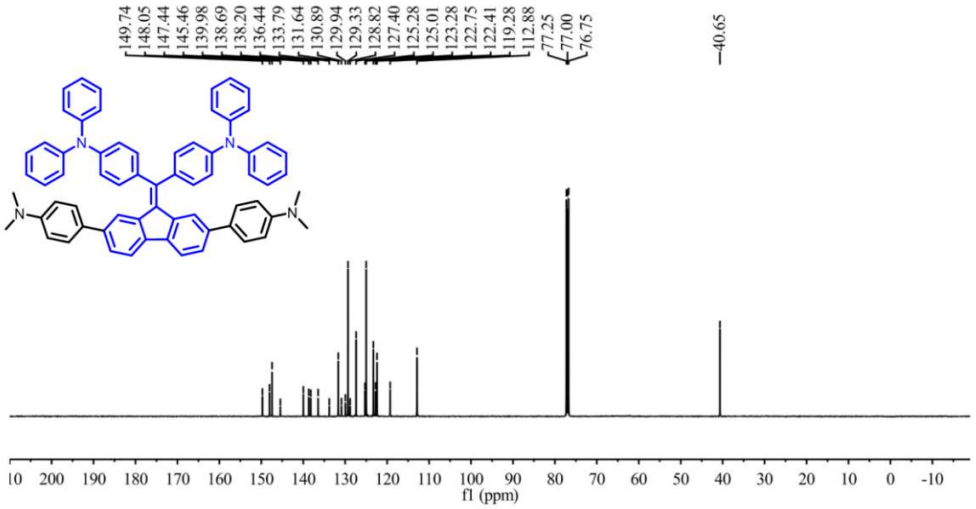

^{13}C NMR spectrum of **Sym-*p*-NMe$_2$**

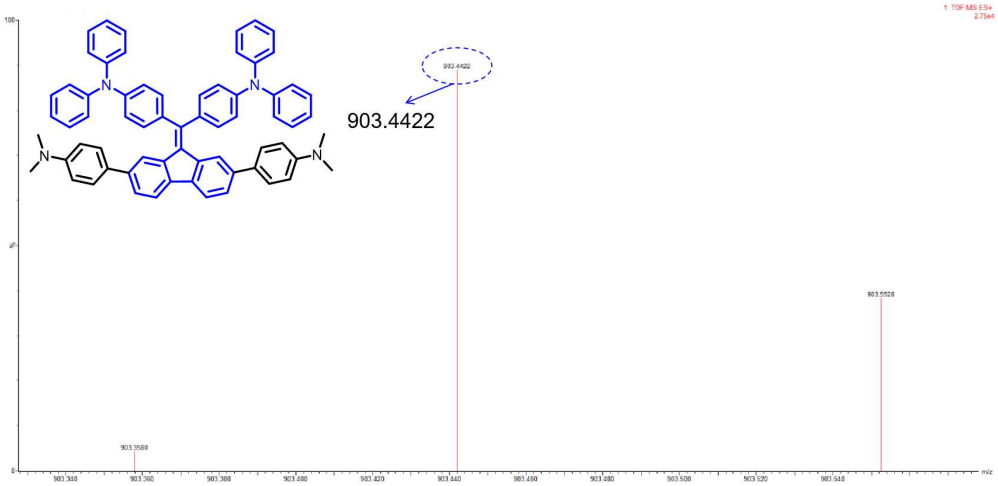

HRMS spectrum of **Sym-*p*-NMe$_2$**

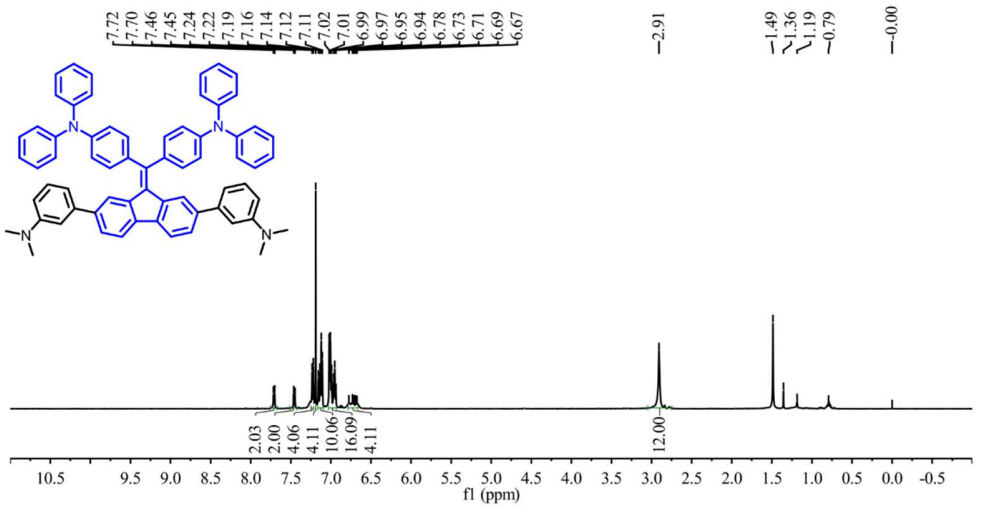

^{1}H NMR spectrum of **Sym-*m*-NMe$_2$**

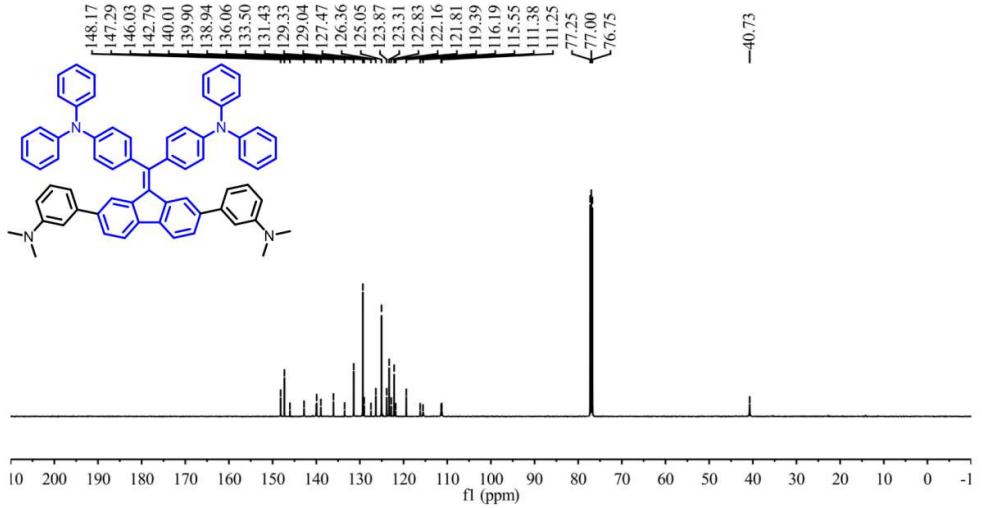

^{13}C NMR spectrum of **Sym-*m*-NMe$_2$**

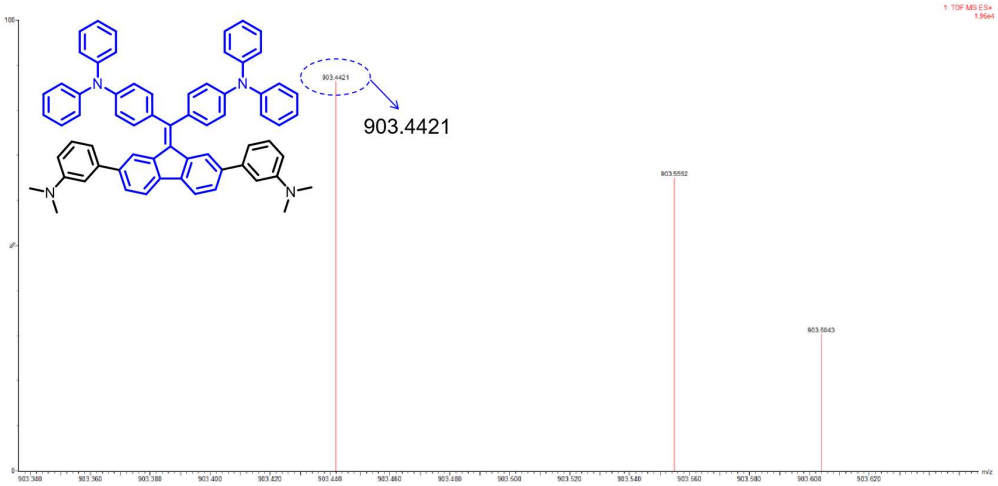

HRMS spectrum of **Sym-*m*-NMe$_2$**

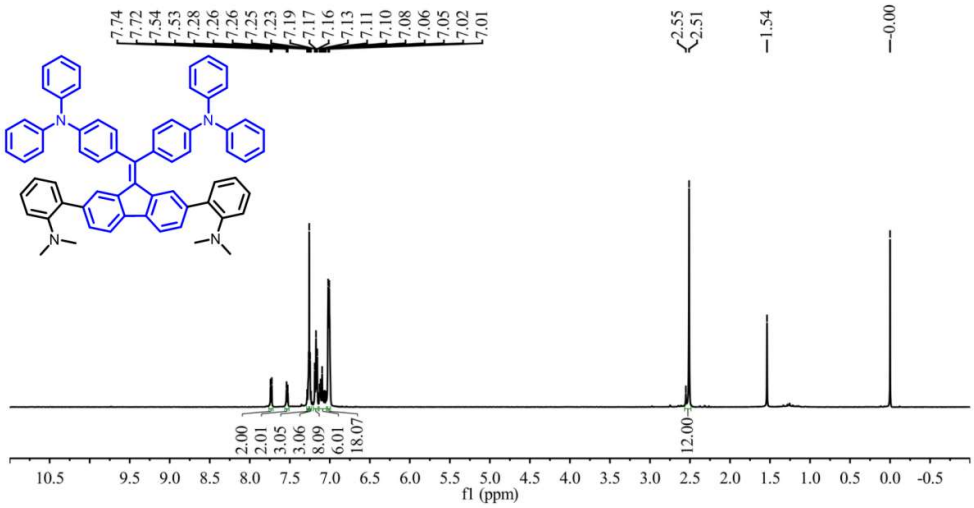

^{1}H NMR spectrum of **Sym-*o*-NMe$_2$**

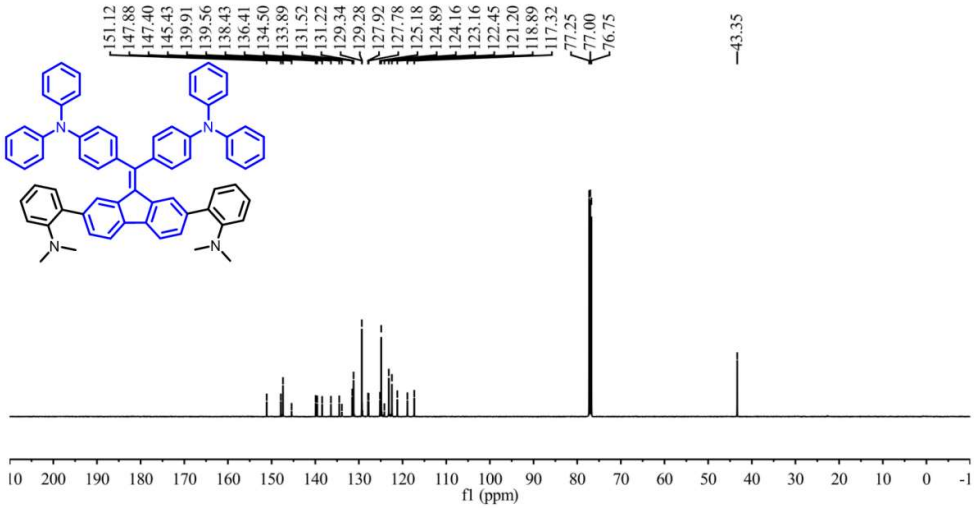

^{13}C NMR spectrum of **Sym-*o*-NMe$_2$**

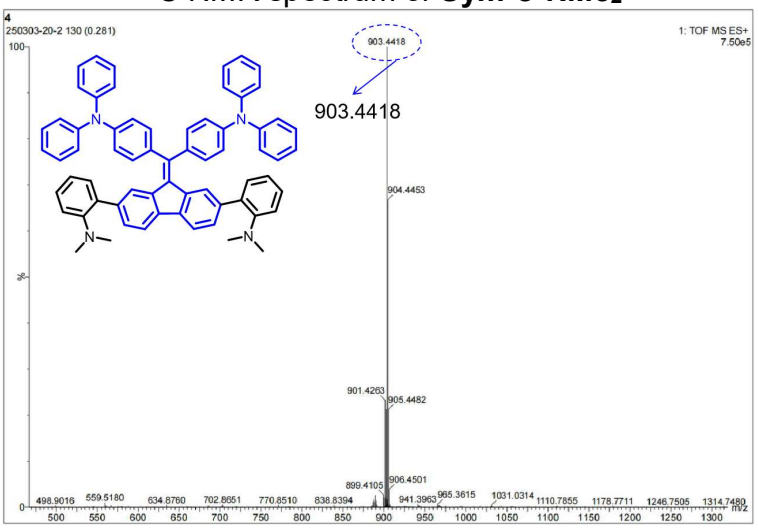

HRMS spectrum of **Sym-*o*-NMe$_2$**

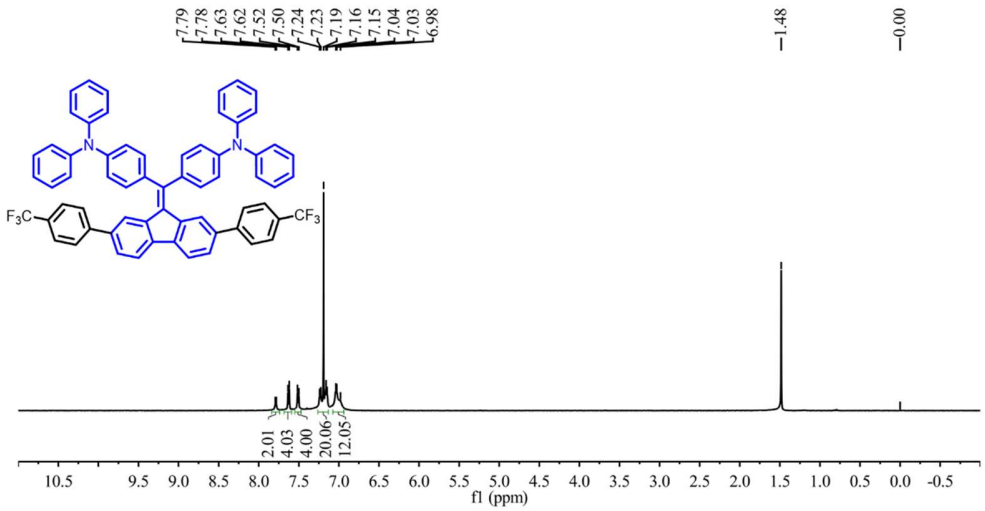

^{1}H NMR spectrum of **Sym-*p*-CF$_3$**

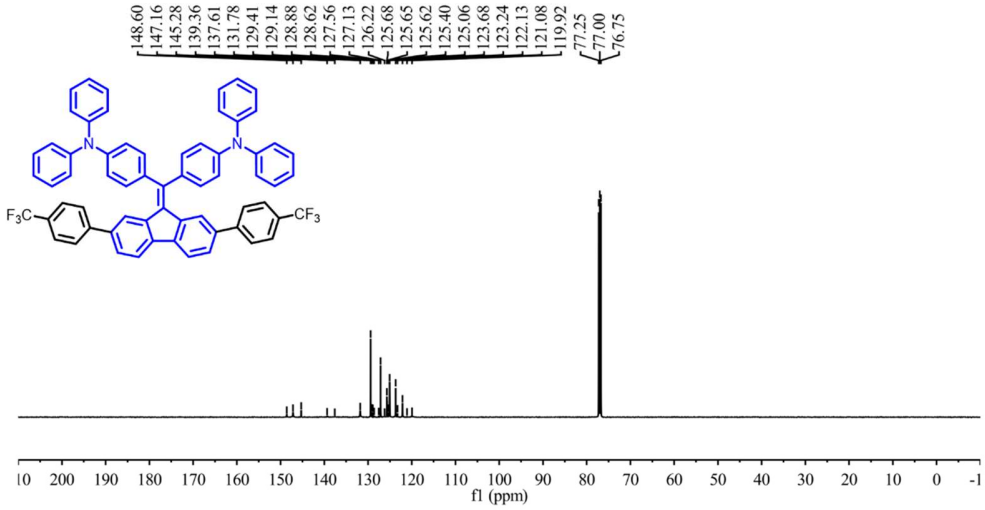

^{13}C NMR spectrum of **Sym-*p*-CF$_3$**

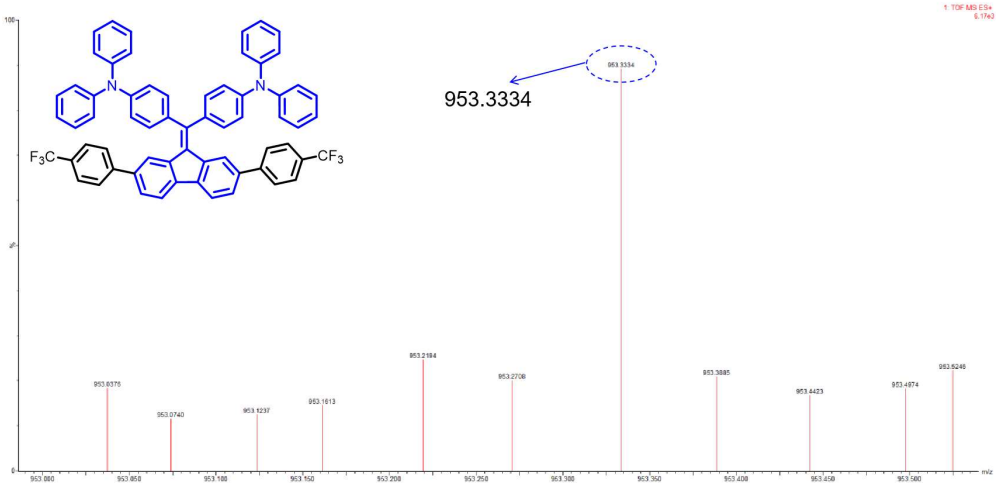

HRMS spectrum of **Sym-*p*-CF$_3$**

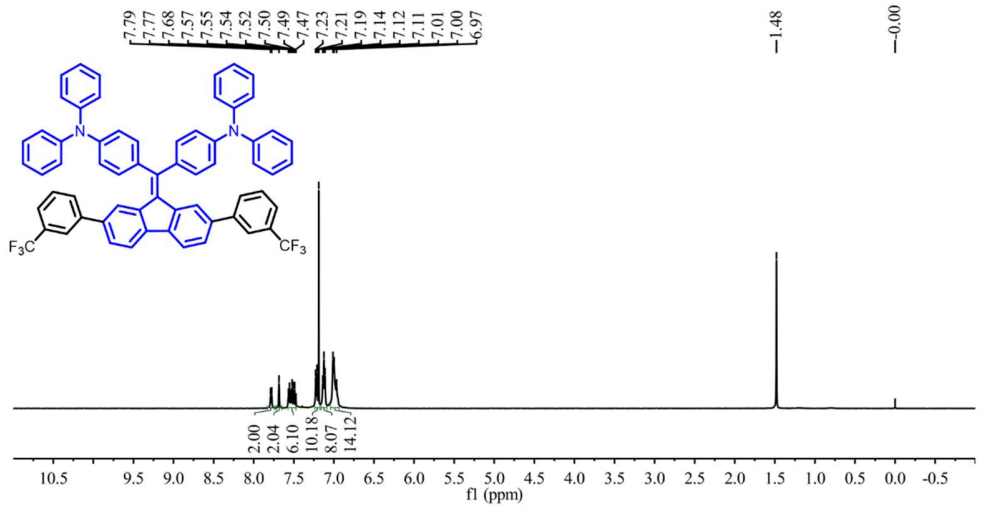

^{1}H NMR spectrum of **Sym-*m*-CF$_3$**

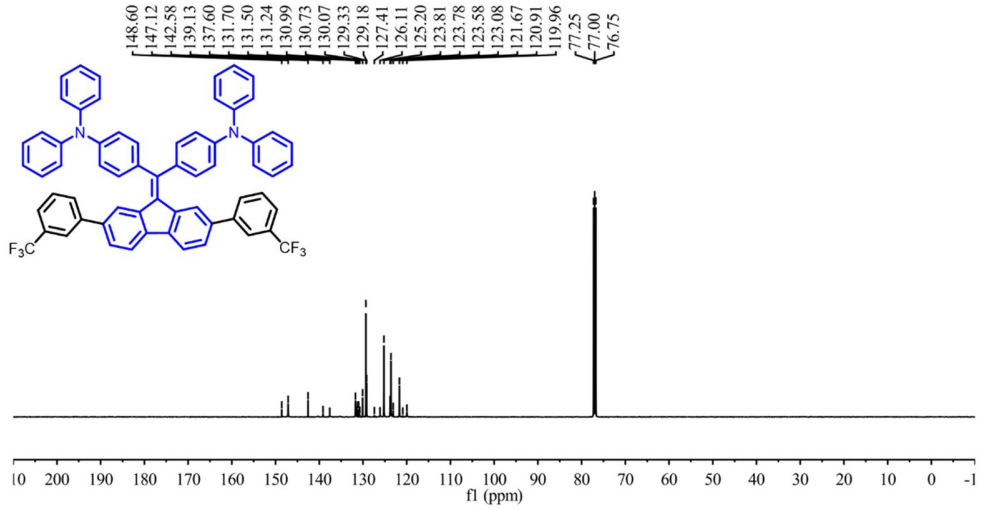

^{13}C NMR spectrum of **Sym-*m*-CF$_3$**

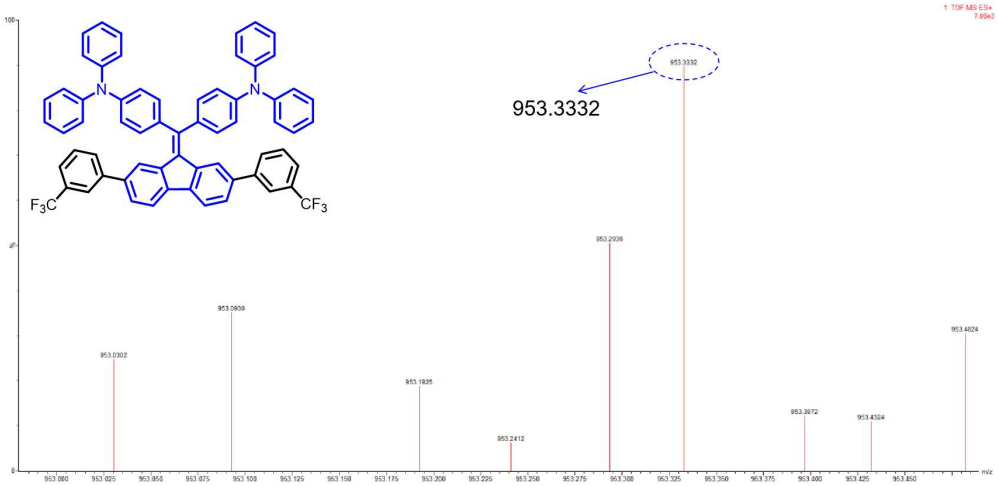

HRMS spectrum of **Sym-*m*-CF$_3$**

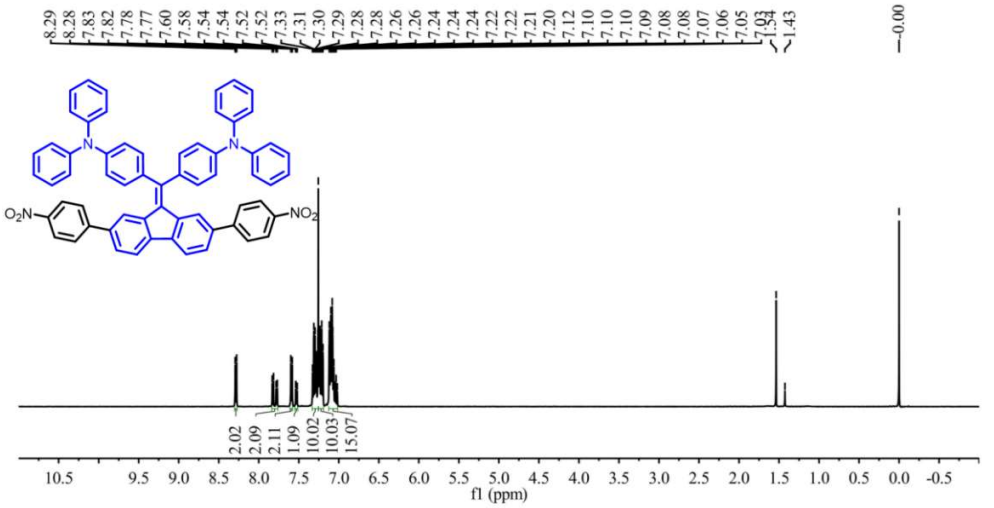

^{1}H NMR spectrum of **Sym-*p*-NO$_2$**

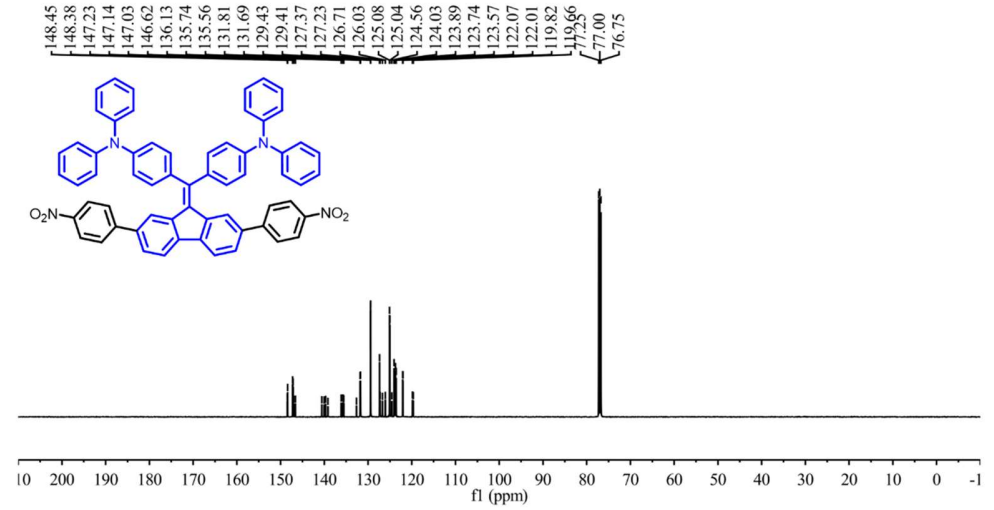

^{13}C NMR spectrum of **Sym-*p*-NO$_2$**

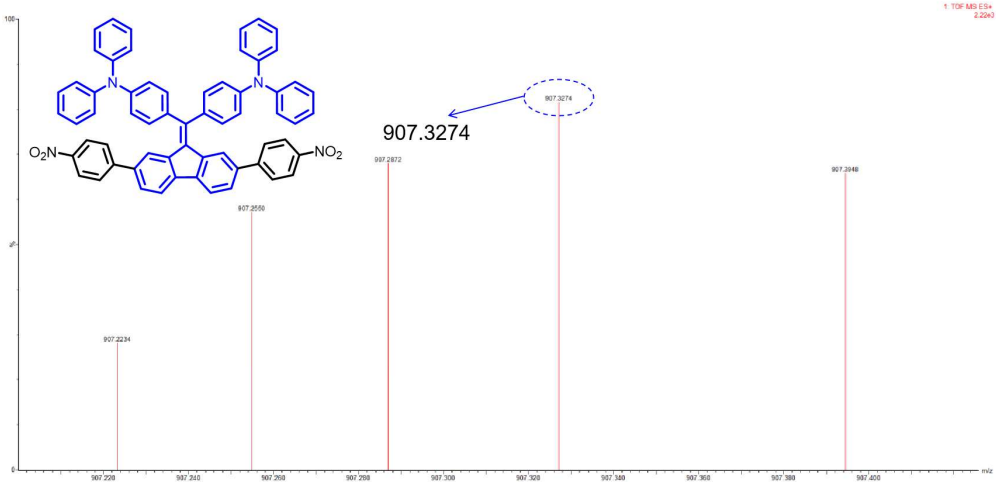

HRMS spectrum of **Sym-*p*-NO$_2$**

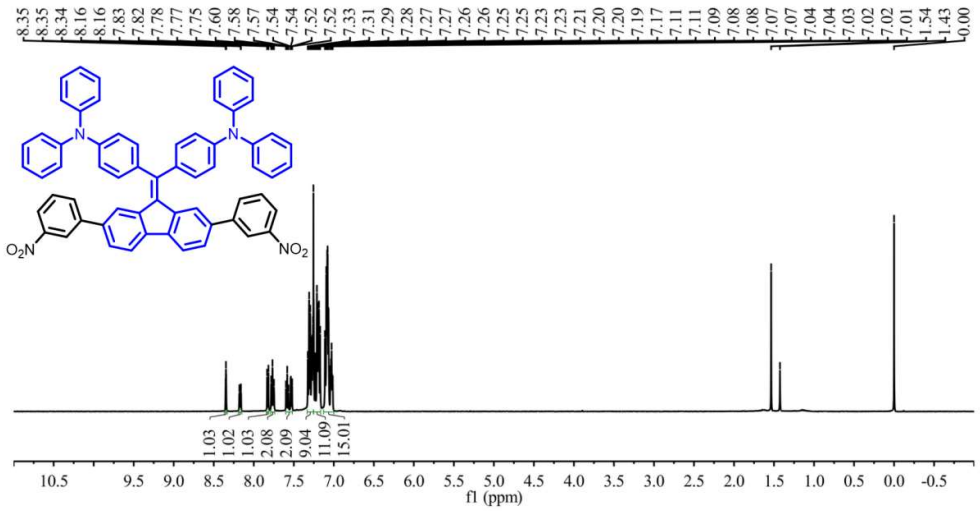

^{1}H NMR spectrum of **Sym-*m*-NO$_2$**

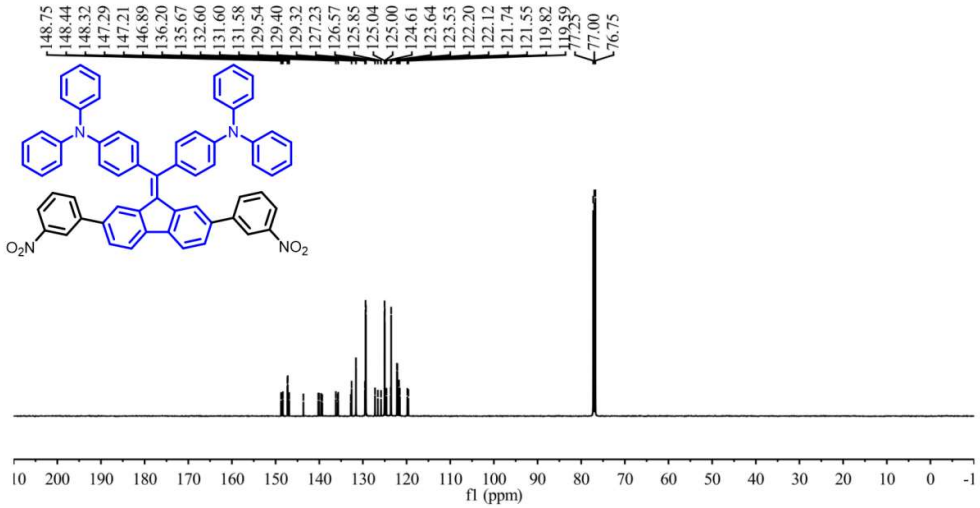

^{13}C NMR spectrum of **Sym-*m*-NO$_2$**

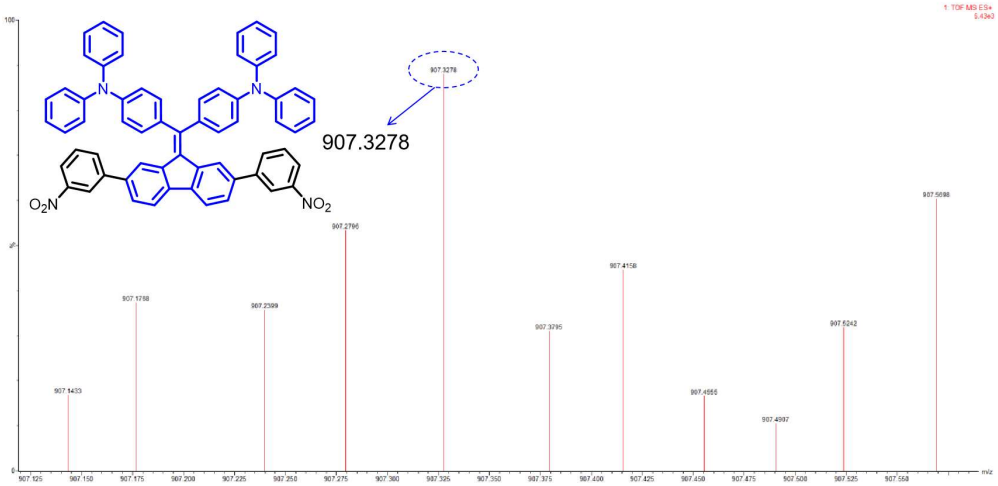

HRMS spectrum of **Sym-*m*-NO$_2$**

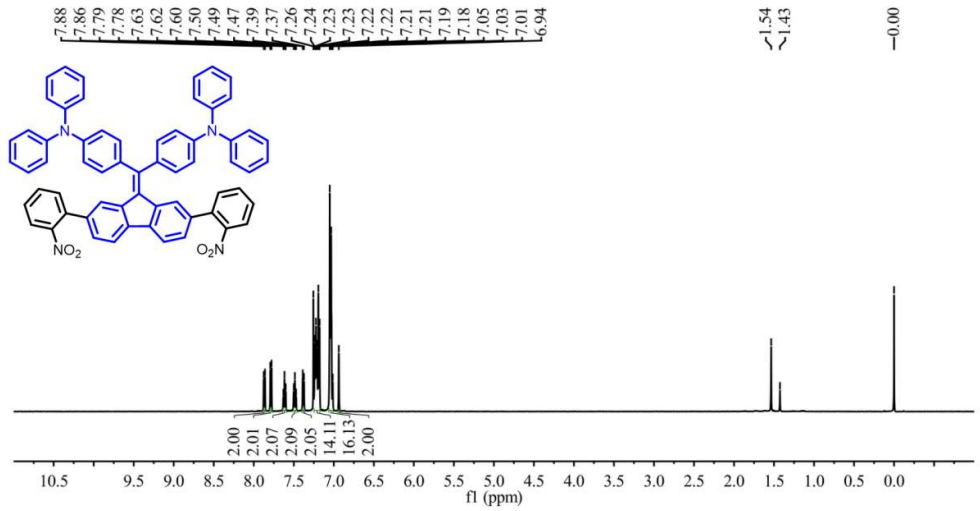

^{1}H NMR spectrum of **Sym-*o*-NO$_2$**

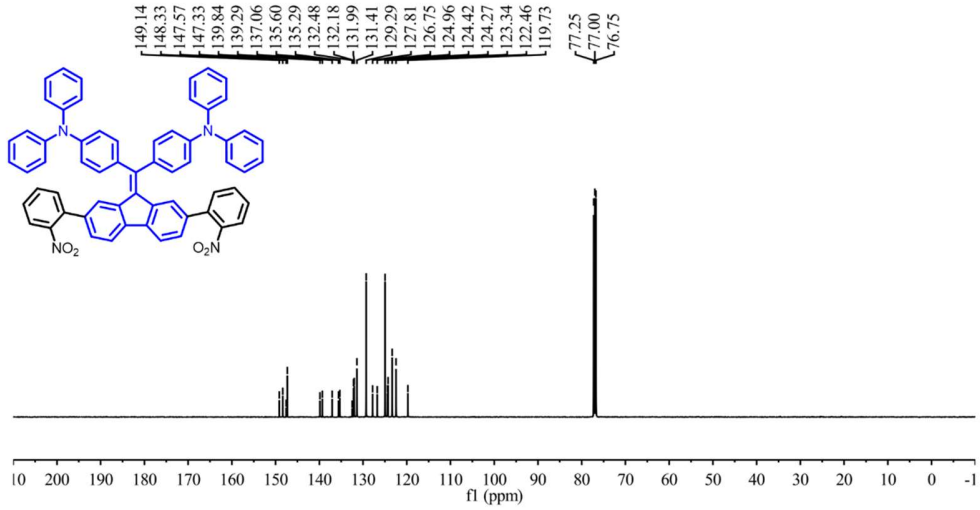

^{13}C NMR spectrum of **Sym-*o*-NO$_2$**

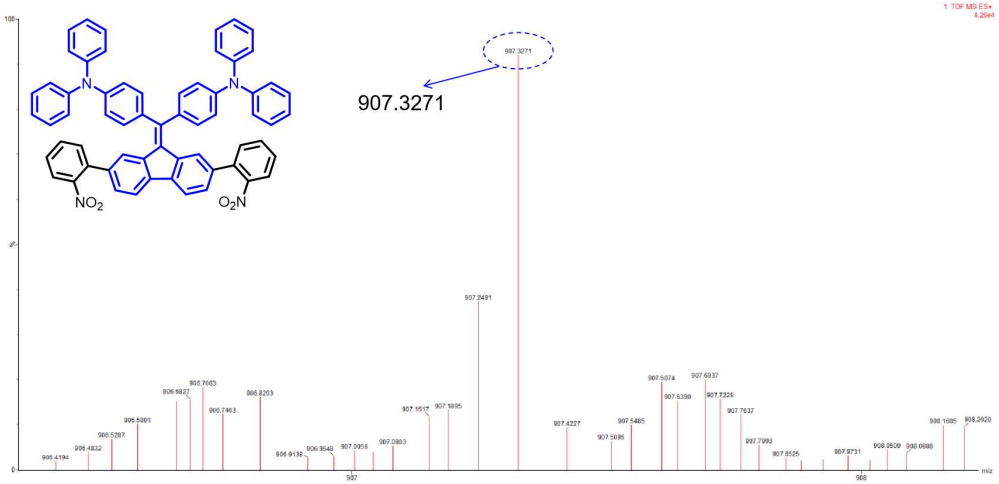

HRMS spectrum of **Sym-*o*-NO$_2$**

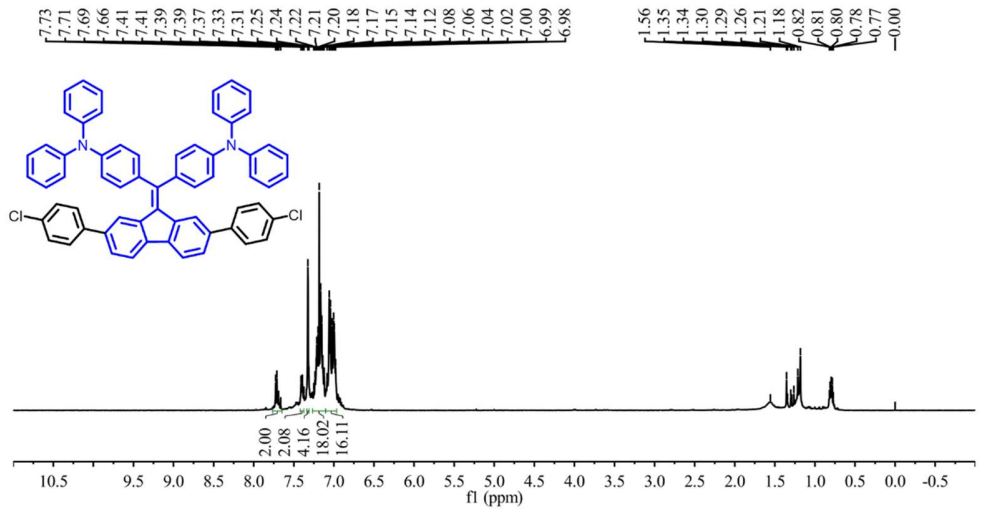

^{1}H NMR spectrum of **Sym-*p*-Cl**

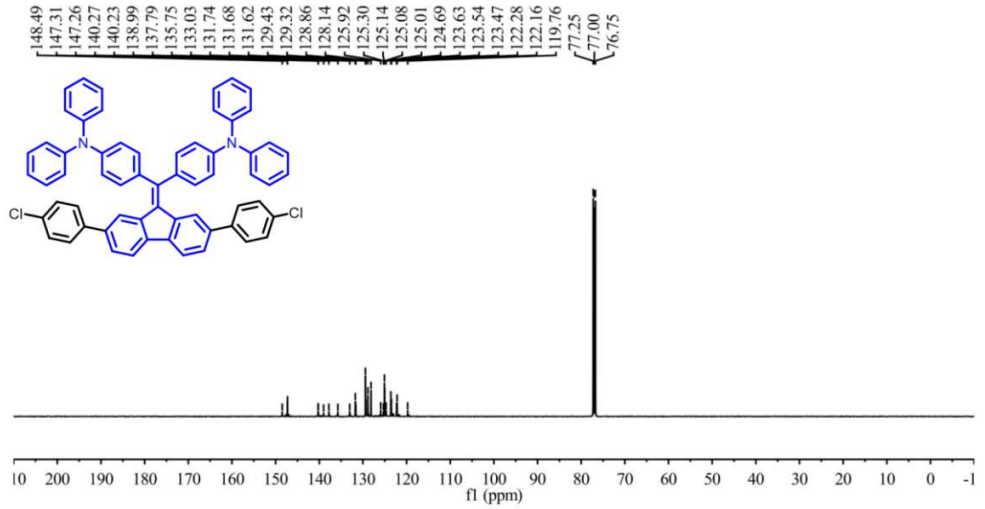

^{13}C NMR spectrum of **Sym-*p*-Cl**

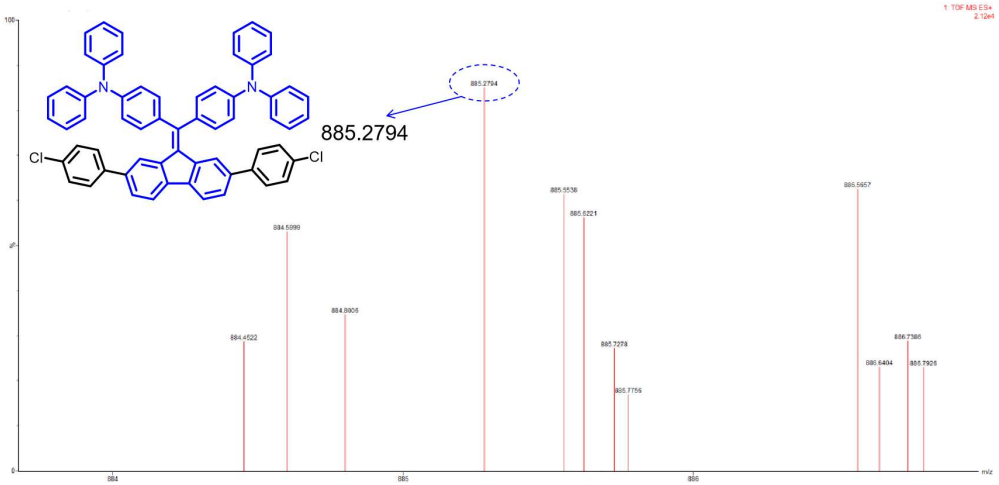

HRMS spectrum of **Sym-*p*-Cl**

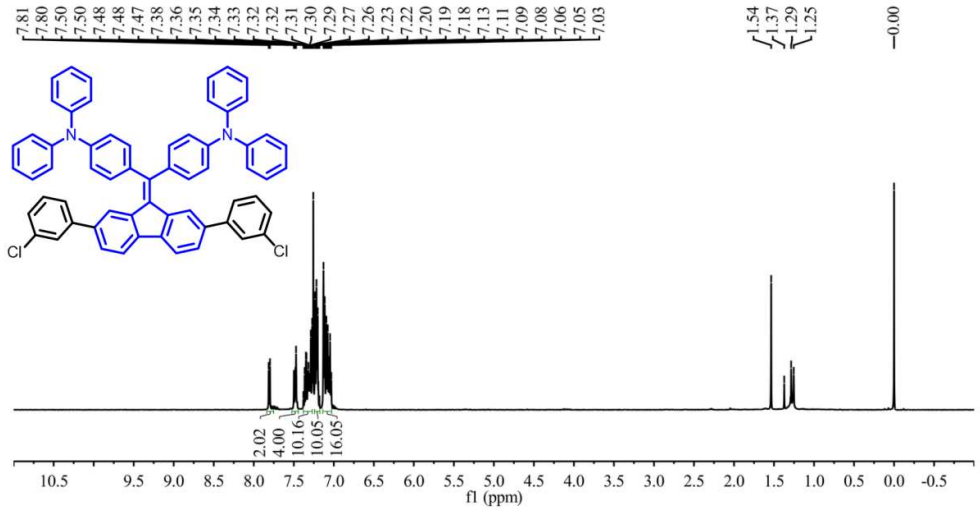

^{1}H NMR spectrum of **Sym-*m*-Cl**

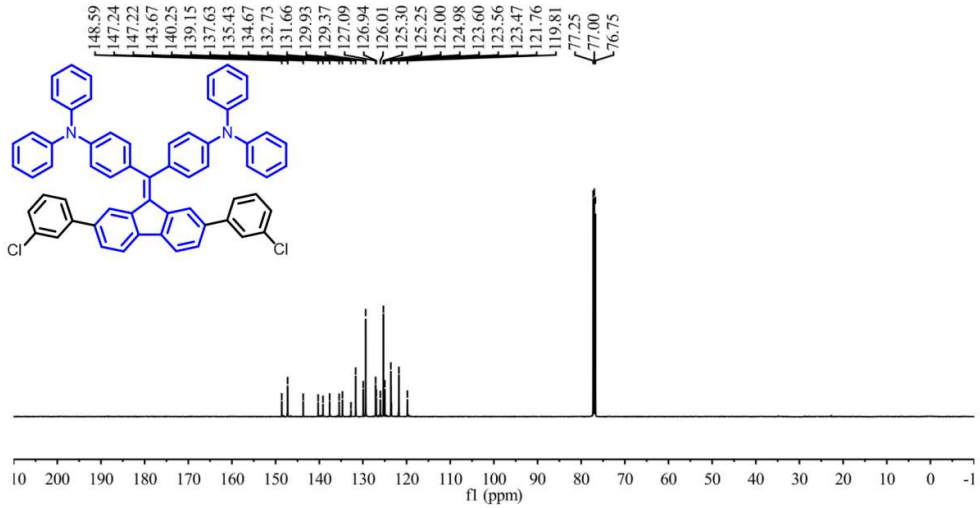

^{13}C NMR spectrum of **Sym-*m*-Cl**

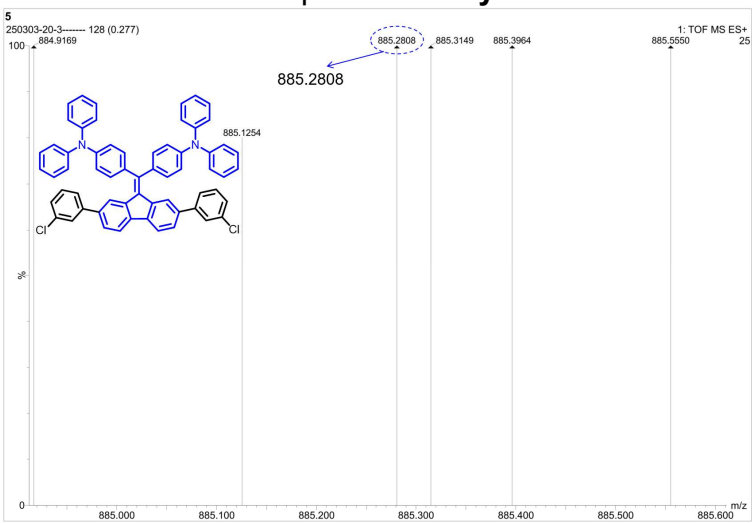

HRMS spectrum of **Sym-*m*-Cl**

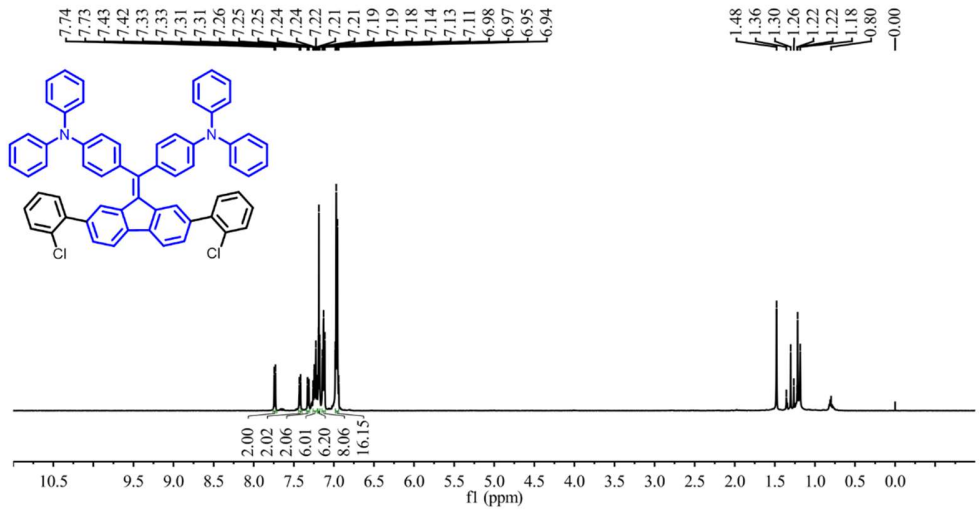

^{1}H NMR spectrum of **Sym-*o*-Cl**

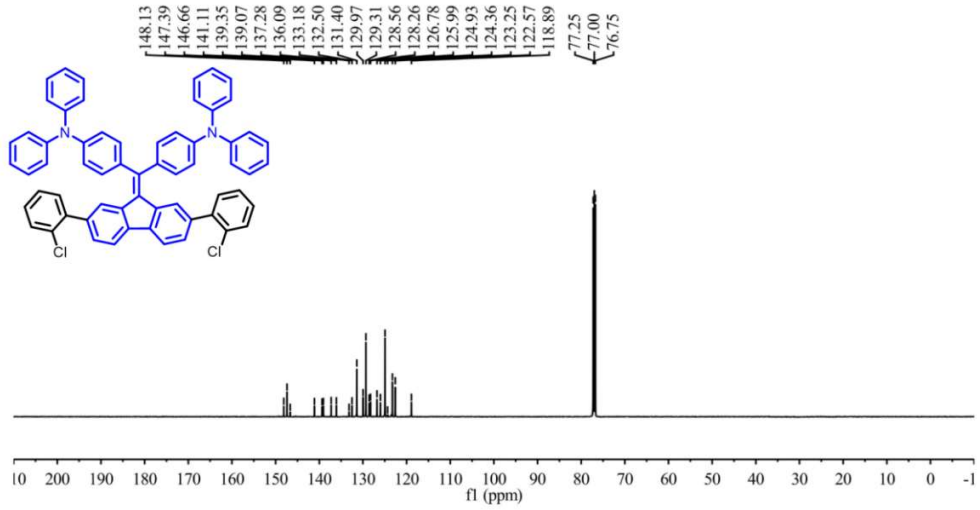

^{13}C NMR spectrum of **Sym-*o*-Cl**

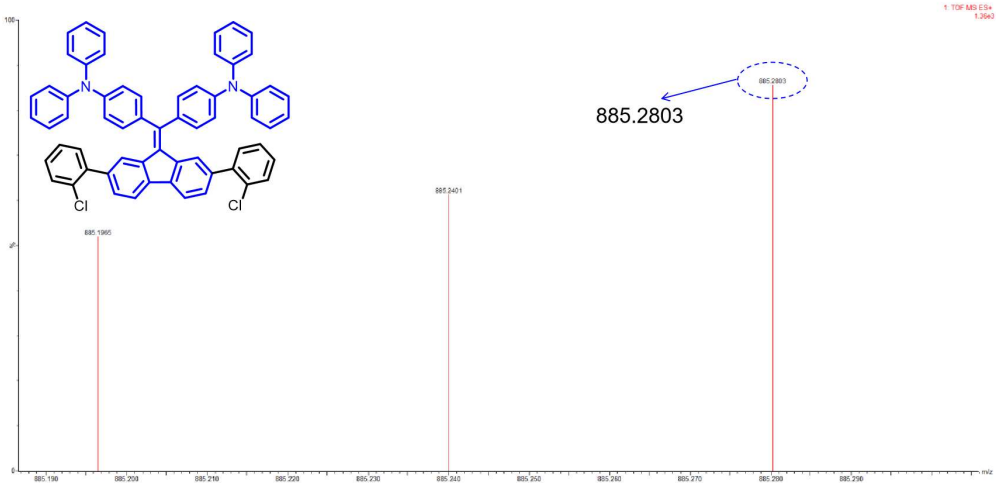

HRMS spectrum of **Sym-*o*-Cl**

19. References

[1] Y. Yin, Q. Guan, Z. Chen, D. Deng, S. Liu, Y. Sun and S. H. Liu, *Sci. Adv.*, 2024, **10**, eadk5444.

[2] P. J. Stephens, F. J. Devlin, C. F. Chabalowski and M. J. Frisch, *J. Phys. Chem.*, 1994, **98**, 11623-11627.

[3] S. Grimme, S. Ehrlich and L. Goerigk, *J. Comput. Chem.*, 2011, **32**, 1456-1465.

[4] W. J. Hehre, R. Ditchfield and J. A. Pople, *J. Chem. Phys.*, 1972, **56**, 2257-2261.

[5] T. Clark, J. Chandrasekhar, G. W. Spitznagel and P. V. R. Schleyer, *J. Comput. Chem.*, 1983, **4**, 294-301.

[6] S. S. Zade, N. Zamoshchik and M. Bendikov, *Acc. Chem. Res.*, 2011, **44**, 14-24.

[7] T. Lu and F. Chen, *J. Comput. Chem.*, 2012, **33**, 580-592.

[8] W. Humphrey, A. Dalke and K. Schulten, *J. Mol. Graph.*, 1996, **14**, 33-38.

[9] Gaussian 16, Revision C.01, M. J. Frisch, G. W. Trucks, H. B. Schlegel, G. E. Scuseria, M. A. Robb, J. R. Cheeseman, G. Scalmani, V. Barone, G. A. Petersson, H. Nakatsuji, X. Li, M. Caricato, A. V. Marenich, J. Bloino, B. G. Janesko, R. Gomperts, B. Mennucci, H. P. Hratchian, J. V. Ortiz, A. F. Izmaylov, J. L. Sonnenberg, D. Williams-Young, F. Ding, F. Lipparini, F. Egidi, J. Goings, B. Peng, A. Petrone, T. Henderson, D. Ranasinghe, V. G. Zakrzewski, J. Gao, N. Rega, G. Zheng, W. Liang, M. Hada, M. Ehara, K. Toyota, R. Fukuda, J. Hasegawa, M. Ishida, T. Nakajima, Y. Honda, O. Kitao, H. Nakai, T. Vreven, K. Throssell, J. A. Montgomery, Jr., J. E. Peralta, F. Ogliaro, M. J. Bearpark, J. J. Heyd, E. N. Brothers, K. N. Kudin, V. N. Staroverov, T. A. Keith, R. Kobayashi, J. Normand, K. Raghavachari, A. P. Rendell, J. C. Burant, S. S. Iyengar, J. Tomasi, M. Cossi, J. M. Millam, M. Klene, C. Adamo, R. Cammi, J. W. Ochterski, R. L. Martin, K. Morokuma, O. Farkas, J. B. Foresman, and D. J. Fox, Gaussian, Inc., Wallingford CT, 2019.

[10] (a) A. D. Becke, *J. Chem. Phys.*, 1993, **98**, 5648-5652. (b) C. Lee, W. Yang and R. G. Parr, *Phys. Rev. B: Condens. Matter Mater. Phys.*, 1988, **37**, 785-789. (c) S. H. Vosko, L. Wilk and M. Nusair, *Can. J. Phys.*, 1980, **58**, 1200-1211. (d) S. Grimme, J. Antony, S. Ehrlich and H. Krieg, *J. Chem. Phys.*, 2010, **132**, 154104.

[11] (a) W. J. Hehre, R. Ditchfield and J. A. Pople, *J. Chem. Phys.*,1972, **56**, 2257-2261. (b) P. C. Hariharan and J. A. Pople, *Theor. Chim. Acta*, 1973, **28**, 213-222.